GA-A15421
UC-77

COMPARATIVE SAFETY ASSESSMENT OF UPFLOW VERSUS DOWNFLOW GCFR CORE DESIGNS

by
M. V. FRANK, C. S. KANG, J. T. REILLY,
and P. A. WHEELER

Prepared under
Contract DE-AT03-76SF71023
for the San Francisco Operations Office
Department of Energy

GENERAL ATOMIC PROJECT 6010
DATE PUBLISHED: SEPTEMBER 1980

GENERAL ATOMIC COMPANY

ABSTRACT

This report presents a hypothetical core disruptive accident safety assessment and a post-accident fuel containment evaluation which were performed at General Atomic Company and contributed to the upflow versus downflow core design decision for the GCFR.

Qualitative and quantitative differences between the upflow and downflow unprotected accident sequences were not significant. However, phenomenological differences manifest themselves when potential accident mitigation and recriticality prevention design concepts are investigated for the loss of shutdown cooling and flow blockage accidents. Duct fallaway in the downflow core could have terminated the loss of shutdown cooling accident with no fuel melting and could have prevented damage propagation from a complete flow blockage of an individual assembly. Drainage through a drain-pipe in an upflow core assembly was found infeasible because recriticality occurs first. Removal of nearly the entire lower axial blanket is required to drain fuel from each fuel assembly. About two metric tonnes of europia are needed to keep a completely slumped core subcritical.

An in-vessel molten fuel containment system is preferred over an ex-vessel system for both the upflow and downflow concepts. The steel bath concept combined with the essential features of a heavy metal bath concept and a crucible concept is considered slightly better than other in-vessel concepts. Both the upflow and downflow PCRV concepts could accommodate a feasible molten fuel containment system with proper design modifications. However, the upflow concept is rated slightly better than the downflow concept because of better fuel containment capability.

CONTENTS

FIGURES

TABLES

1. SUMMARY AND CONCLUSIONS

This report presents the evaluations and analyses of a hypothetical core disruptive accident (CDA) safety assessment and a post-accident fuel containment (PAFC) evaluation which were performed at General Atomic Company and contributed to the upflow versus downflow core design decision for the gas-cooled fast breeder reactor (GCFR). Five elements were considered in the assessments:

1. Determination of the sequence of events in an unmitigated loss of shutdown cooling (LOSC) accident.

2. Determination of the feasibility of LOSC recriticality prevention concepts.

3. Assessment of the flow blockage accident.

4. Assessment of the unprotected transient overpower (TOP) accident.

5. Assessment of the PAFC capability.

1.1. LOSC EVENT SEQUENCE

Detailed core heatup and recriticality calculations were performed to determine the core heatup sequence, cladding and fuel melting rates, and time of criticality for an LOSC accident. In general, the accident proceeds in seven chronologically and phenomenologically distinct phases: (1) initiation, (2) cladding melting, (3) duct wall melting, (4) fuel melting, (5) recriticality, (6) transition, and (7) PAFC.

The core heatup analysis did not include convection effects in the central cavity. This omission tended to underestimate the calculated time of recriticality. However, the time of recriticality is also very sensitive to the particular assumptions of molten fuel spreading over a single assembly and from one assembly to another. In general, spreading a molten fuel layer over more assemblies reduces the criticality. It was assumed the molten fuel would spread uniformly over adjacent circumferential rings of assemblies. This tended to overestimate the calculated recriticality time. Hence, the calculated time of 970 s should be considered a best estimate. Central cavity convection would also raise the prestressed concrete reactor vessel (PCRV) pressure and might cause relief valve opening prior to cladding melting. This effect was not assessed. The specific results presented in this report should be regarded as best estimates to date. The most important conclusions are as follows:

1. The unmitigated differences between the LOSC sequence of events for the upflow and downflow cores (without including design specifically developed for accident mitigation) are found in the quantifiable details. Major phenomenological differences in the inherent core response to the accident initiator have not yet been identified.

2. However, certain phenomenological differences in core response to the initiator occur among design concepts specifically developed for accident mitigation and recriticality prevention.

3. Multiple criticality events are not certain, nor can they be ruled out. Fuel boilup will not prevent recriticality for pressurized cases and may not for depressurized cases at low decay heat. The energetics of multiple recriticalities are not known, and a calculated core fraction vaporization limit cannot be established yet. Future work should focus on establishing the unmitigated limit and minimizing the potential for recriticality.

1.2. LOSC CONSEQUENCE MITIGATION

Mechanisms and design concepts which might prevent recriticality during an LOSC accident were investigated. The following mechanisms were evaluated for both the upflow and downflow cores:

1. Adding sufficient neutron absorber material which is soluble in molten fuel (poison concept).

2. Draining molten fuel through the lower axial blanket and out of the bottom of each fuel assembly (internal drainage concept).

3. Draining sufficient molten fuel out of the core and blankets through special control assemblies in a timely manner to prevent recriticality (external drainage concept).

In addition, duct fallaway was investigated for the downflow core. The conclusions are presented in Table 1-1. A combination of an external drain concept and a poison concept may also be feasible. The condition for feasibility would be to delay criticality by poison addition long enough to allow fuel drainage through control assemblies. Further work on combining drains with poison may be warranted. The internal drainage concept is technically feasible but requires the elimination of practically the entire lower axial blanket in most of the core assemblies. The only feasible recriticality prevention concept with reasonable design impact discovered to date is duct fallaway for the downflow core. The principal concerns are neither the ability of ducts to fall nor the holdup of ducts by adjacent assemblies, but the potential for fuel-crumbling-induced criticality before fallaway.

1.3. ASSESSMENT OF FLOW BLOCKAGE ACCIDENT

A complete flow blockage in a single assembly was investigated to determine the potential for damage propagation to neighboring cooled

TABLE 1-1
ASSESSMENT OF LOSC CONSEQUENCE MITIGATING FEATURES

	Concept			
	Poison Solution	Internal Drainage	External Drainage	Duct Fallaway (Downflow Only)
Technical feasibility	Yes	Yes	No, recriticality occurs first	Yes
Design penalty	Moderate: poison stored in upper axial blanket	Very large: no lower axial blanket	—	Small: low friction duct treatment or increased gap between assemblies
Prerequisites	An appropriate, reliable initiation mechanism	No fuel crumbling recriticality	—	No fuel crumbling recriticality
Testability	Fair: 7 to 37 rods in-pile or in an out-of-pile meltdown test	Fair: full size out-of-pile with heater development or a thermite process; 37 rods in-pile in GRIST-2	—	Good: fuel size out-of-pile DMFT; fuel crumbling with 37 rods in GRIST-2 or out-of-pile with heater development

assemblies. Cladding melting leads to a blockage in the lower axial blanket of the blocked assembly similar to that in the LOSC accident. However, in contrast to the LOSC accident, fuel melting and slumping precede duct wall melting. Substantial fuel melting would precede reactor trip. A molten fuel pool with temperatures a few hundred degrees above the liquidus would collect on the steel blockage and begin melting the duct wall as the reactor power and flow rate decreased after trip. Within a few tens of seconds, the molten pool in an upflow core is calculated to melt through the duct wall of a neighboring assembly despite a continued, albeit decaying, flow rate. (The average post-trip flow rate is 10% of full flow.) This sequence would lead to welding together of the seven-assembly group which had the blocked assembly at its center. The relatively short time between detection and damage propagation appears to preclude operator intervention. However, in principle, a minimum residual flow rate exists for which the assembly wall adjacent to the blocked one would not melt.

A downflow core designed for fallaway during an LOSC accident would automatically provide an early accident termination mechanism without damage propagation. When the molten pool raised the duct wall temperature to its yielding point under the assembly weight, the assembly would drop from the core. This would occur before melting of neighboring assemblies.

1.4. UNPROTECTED TRANSIENT OVERPOWER (TOP) ACCIDENT

The TOP accident has been qualitatively investigated with respect to flow direction and support direction. A qualitative analysis has determined that the TOP consequences are insensitive to flow direction and ought to be substantially less than those of an unprotected loss of flow. The key uncertainties in TOP consequence determination are cladding failure location, fuel particle sweepout from the core, and primary side damage from dispersed fuel.

1.5. UNPROTECTED LOSS OF FLOW ACCIDENT

The loss of flow (LOF) accident has been qualitatively investigated with respect to flow direction and support direction. The major qualitative difference appears to be the influence of residual coolant flow on molten fuel and cladding motion. Less significant differences are the potential for fuel removal above the core and fuel freezing and plugging below the core. Quantitative estimates have been performed at Argonne National Laboratory and are not reported herein.

1.6. PAFC CAPABILITY

The upflow and downflow designs for the 300-MW(e) GCFR were evaluated and compared with regard to PAFC requirements. Supporting analyses are presented herein. Conclusions from the evaluations are:

1. An in-vessel molten fuel containment system (MFCS) is technically preferred to an ex-vessel system for both the upflow and the downflow designs principally.

2. For an in-vessel system, several diverse PAFC concepts are feasible. The steel bath concept combined with the essential features of other concepts is slightly better than other concepts.

3. No major feasibility problems with PAFC have been identified for any of the concepts to date. Both the upflow and downflow designs could be made feasible with proper design modifications.

4. A technical concern is the unavailability of the MFCS during refueling for the downflow design or during fuel spillover for the upflow design.

5. The upflow design is rated slightly higher than the downflow design because of better fuel contaiment capability.

2. INTRODUCTION

In April 1979, the GCFR reference design was changed from a top-supported downflow core to a bottom-supported upflow core. The predominant reason was to provide the capability for pressurized decay heat removal by natural coolant circulation from the core to the ultimate heat sink. This report presents a hypothetical CDA safety assessment and a PAFC assessment which were performed at General Atomic Company and contributed to the design change decision. A complementary study was performed at Argonne National Laboratory but is not reported in this document.

The first part of this report describes and quantifies an accident sequence initiated by a loss of all forced circulation and the postulated failure to establish natural circulation in a shutdown reactor. It has been named the loss of shutdown cooling accident, or LOSC. Some conceptual work on this accident in downflow core design has been previously reported (Refs. 2-1, 2-2). The hypothetical accident sequence is described in three sections: initiation through recriticality, transition phase, and PAFC. Initiation through recriticality would occur in four phases: cladding melting, duct wall melting, fuel melting, and recriticality.

The second part of this report compares the responses of the upflow and downflow designs (as described in Ref. 2-3) to three accidents:

1. The LOSC accident.

2. A postulated complete flow starvation of an individual fuel assembly (flow blockage accident).

3. A postulated reactivity ramp insertion at full power without reactor scram (TOP accident).

Several major differences exist between the upflow and downflow GCFR designs which are relevant to PAFC capability. The most important are the direction of helium flow, the location of the refueling penetration into the PCRV, the location of the core relative to the core support plate, and the location of shielding materials. These aspects were evaluated for both the upflow and downflow designs. Early PAFC studies are reported in Ref. 2-4. Several additional analyses of in-vessel and ex-vessel MFCS concepts are presented herein. These include evaluations of each concept in comparison with the others and an evaluation of in-vessel versus ex-vessel molten fuel containment.

REFERENCES

2-1. Torri, A., and D. R. Buttemer, "Loss of Flow Accident Phenomenology in the GCFR," ANS Trans. 21, 295 (1975).

2-2. Torri, A., and J. L. Tomkins, "Accident Termination by Element Dropout in the GCFR," Proceedings of the Fast Reactor Safety Meeting, Chicago, October 1976, pp. 1183-1194.

2-3. Menzel, H. F. (ed.), "GCFR Upflow/Downflow Study Summary Report," DOE Report GA-A15455, General Atomic Company, August 1979.

2-4. Kang, C. S., and A. Torri, "Preliminary Analysis of Post-Accident Fuel Containment for a GCFR," DOE Report GA-A14789, General Atomic Company, to be published.

3. LOSC EVENT SEQUENCE DESCRIPTION

3.1. INITIATION PHASE

The postulated LOSC accident has several characteristics which would be distinctly different from loss of flow accidents initiated at full power and without scram. The initial fuel heating rates would be dominated by decay heat. Therefore, the time scale of melting would be two to three orders of magnitude longer. At the time of initial fuel melting, the reactor would be shut down and delayed neutron precursor concentrations would be orders of magnitude smaller. Therefore, larger amounts of reactivity could be inserted before fission power became a significantly greater heat producer than decay heat and before Doppler feedback became important. Furthermore, as fission power increased, the neutron spectrum would be harder because of the control rod insertion and nearly complete decladding of fuel rods. Hence, the Doppler coefficient would be smaller than in the unprotected case.

The initiating event phase of the LOSC accident sequence requires a series of common mode failures to be postulated that leads to a total loss of decay heat removal. The reference scenario considered for analysis of the core melting progression postulates the following occurrences for the downflow core:

1. A simultaneous loss of all drive power to the electrically driven main circulators is assumed to occur as the initiating event.

2. A common mode failure of the main circulator pony motors is postulated to cause failure of the shutdown cooling system when main circulators have coasted down to the pony motor design speed.

3. Common mode failure of the core auxiliary cooling system (CACS) to energize is postulated to disable the CACS forced convection cooling mode.

The upflow core provides the capability for pressurized decay heat removal by natural coolant circulation from the core to the ultimate heat sink. Therefore, an LOSC accident would not occur in an upflow core unless:

4. As common mode failure is postulated to prevent the removal of decay heat by natural circulation.

3.2. DAMAGE PHASE

The hypothetical accident description herein is substantially the same for either the upflow or downflow design. Numerical details are slightly different, but major phenomenological differences have not yet been identified. The major differences arise from the potential success of design modifications to avoid recriticality. Cladding and assembly wall melting is expected within several minutes in the absence of loop coolant circulation under decay heat generation because of the limited core heat capacity. The accident sequence summarized in Fig. 3-1 and the phenomenological event timing in Fig. 3-2 are based on neglecting inter-assembly and intra-assembly natural convection in an upflow GCFR core. These will be included in future analyses. The accident sequence is substantially the same whether the reactor is tripped by the engineered plant protection system signals or is already shut down when circulator coast-down begins. However, the length of time between each significant event is extended as the loss of flow is delayed after shutdown.

Based on experimental observations in experiments FLS-1 and FLS-2 at Los Alamos Scientific Laboratory (LASL), a substantial delay in the time

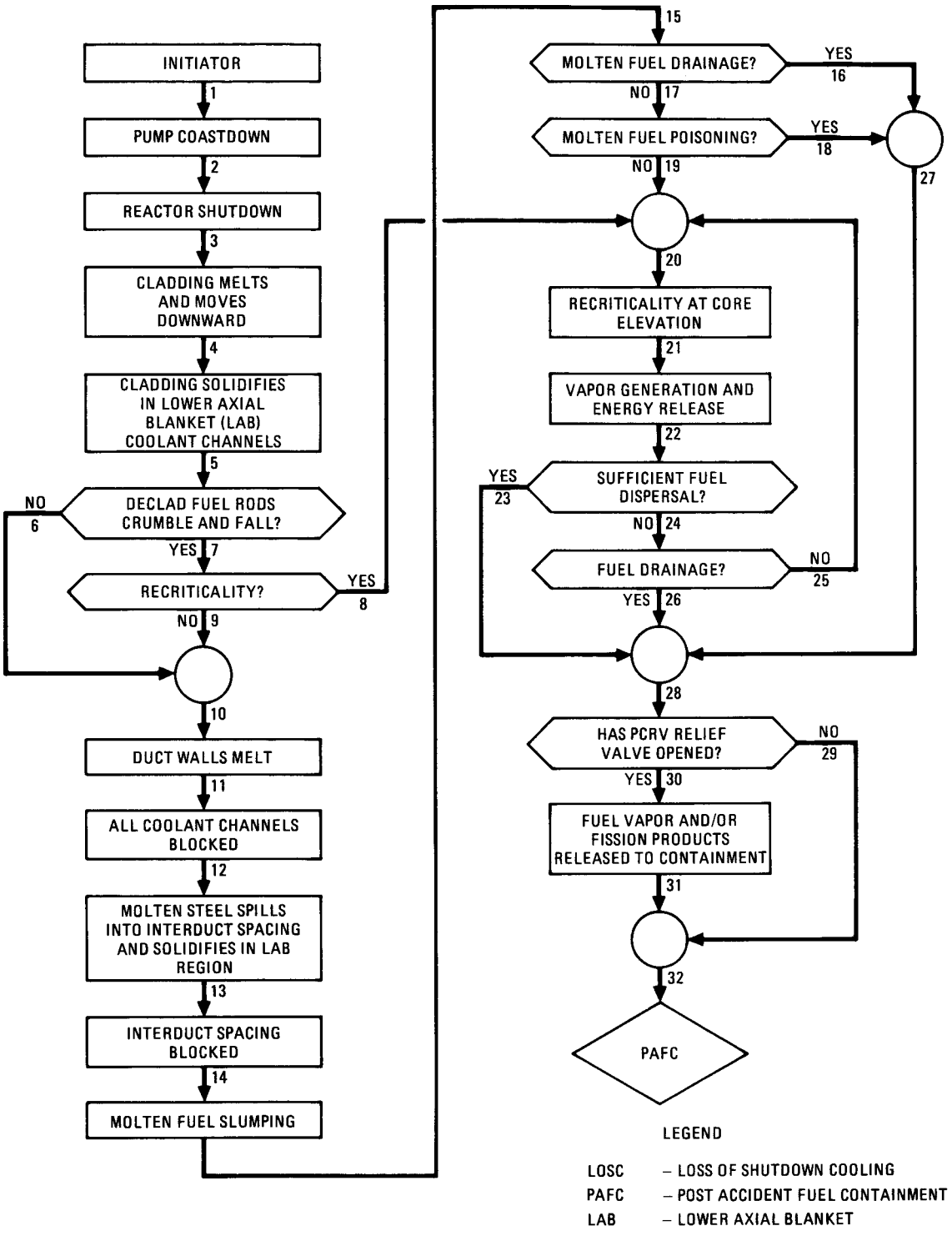

Fig. 3-1. LOSC event sequence diagram for an upflow core (pressurized case)

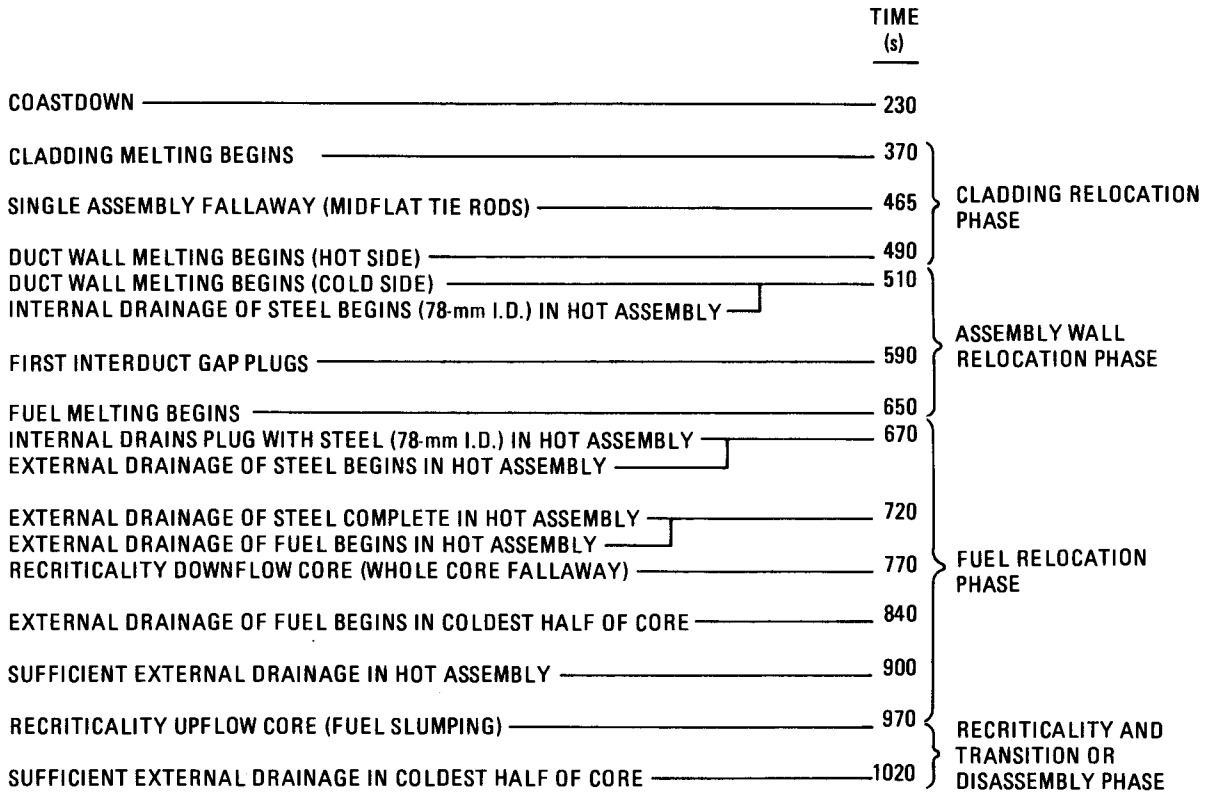

Fig. 3-2. LOSC phenomenological event timing

of cladding melting is expected owing to natural circulation heat transport from the core to the upper plenum structures. Natural convection is expected to continue even after cladding melting. Therefore, a delay in the fuel melting time is also expected.

The accident proceeds in five phenomenologically and chronologically distinct phases (Fig. 3-2):

1. Cladding relocation.
2. Assembly wall relocation.
3. Fuel relocation.
4. Recriticality and transition or disassembly.
5. PAFC.

The quantitative results should be considered approximate subject to the above qualifications.

Approximately 6 min after a postulated simultaneous reactor trip and circulator trip, the cladding begins to melt. It relocates downward and has been calculated to refreeze in the lower axial blanket near the core bottom. Nearly all lower axial blanket coolant channels may be blocked by this process. Only those adjacent to the assembly walls are calculated to remain partially open at this time. In the hottest rod of the core, the cladding melts over 50% of the core length in 20 s.

Exposure of the assembly walls to thermal radiation from the declad fuel columns causes them to melt at the hottest axial level about 2 min after incipient cladding melting. Melting of a duct wall adjacent to a control rod assembly (cold side) is delayed about 20 s relative to wall melting adjacent to a fuel assembly. The axial progression of melting along the hexagonal assembly wall flat is initially faster than the circumferential progression (Ref. 3-1). The added molten steel inventory blocks the remaining lower axial blanket coolant channel. The modeling presumes

that melting of the assembly walls also results in a buildup of relocated steel which solidifies on the assembly wall over the lowest 200 mm of the core. This results in a steel "cup" in each assembly. The bottom of the cup is a platform of solidified cladding in the lower axial blanket reaching to the core/blanket interface. The sides of the cup are solidified assembly wall steel and unmelted assembly wall. This buildup of steel retards the axial progression of the assembly wall melt front. As the assembly walls continue to melt, the molten steel flows into this cup, forming a molten steel pool. Continued addition of molten steel backfills the cup until the pool spills over the sides and into the interassembly spacing. Assembly wall melting, pool buildup, and spillover are illustrated in Fig. 3-3. The spilled steel is calculated to solidify near the core bottom in the lower axial blanket region of the interassembly spacing. There is sufficient molten steel inventory to completely block the spacing around the hexagonal assembly.

Between the time that the rods become declad and the beginning of fuel melting, the fuel columns are left without their cladding restraint. One early mode of fuel relocation which may induce criticality is the crumbling and compacting of fuel columns. One cause of crumbling may be stresses induced by bowing of fuel columns near the assembly walls and subsequent mechanical interaction of fuel columns with the wall and each other. The cause of bowing is a temperature gradient across rods near the assembly wall. Fission-gas-induced solid fuel swelling under substantially isothermal heatup conditions in central rods may tend to stabilize the declad fuel columns.

Fuel melting commences after most of the assembly walls have melted, assuming the fuel columns did not crumble. The molten fuel is assumed to slump into the steel-formed cups and settle upon the solidified steel platform. The molten steel is assumed to be displaced upward, hence contributing to steel spillover. Fuel which continues to slump increases the pool height. When the surface of the steel pool reaches the hole melted

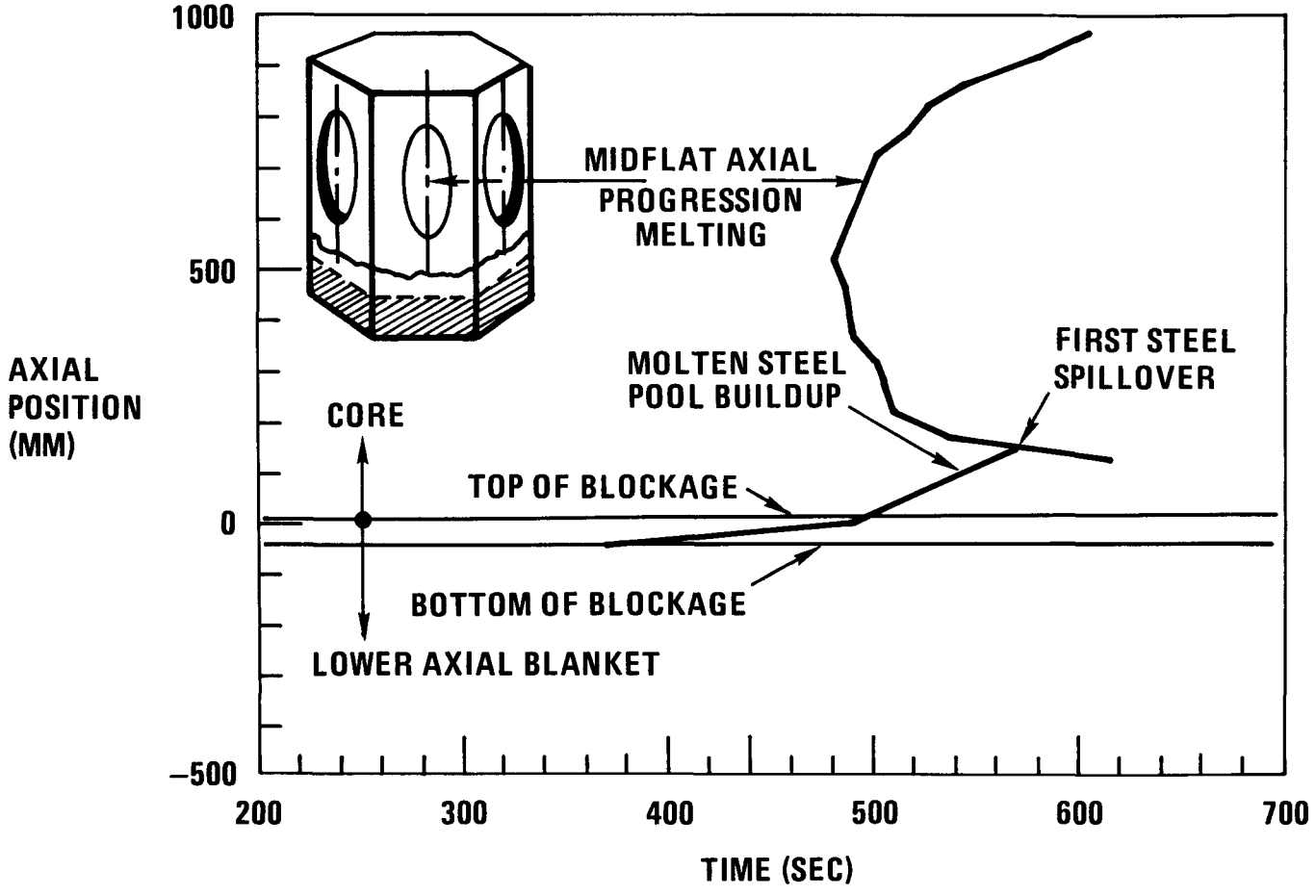

Fig. 3-3. Assembly wall melting, pool buildup, and spillover

in the assembly wall of the adjacent assembly, steel spills over into that assembly. The molten fuel follows the molten steel until an equilibrium height is reached. Steel vaporization is not expected to occur because the 8.8-MPa system pressure raises the steel vaporization temperature to over 4500 K (Ref. 3-2), approximately that of fuel. The decay heat generation at this time is too low to produce boiling of fuel or steel with the maximum achievable pool height for criticality. The high pressure will also limit fission gas volume fractions within the molten fuel. Eventually, the assembly walls and solidified cladding completely melt down to the core bottom. The molten fuel and steel are assumed to uniformly spread over all such assemblies so that a molten fuel layer is between a molten steel layer above and steel-blocked lower axial blanket below. The sections of melted fuel columns above and below the central molten region are assumed to join so that a void space (filled with helium) is left between the top of the unmelted fuel columns and the upper axial blanket.

Approximately 5 min after incipient fuel melting, enough fuel to overcome the shutdown margin will have slumped and compacted upon the lower axial blanket blockage. The approach to a critical configuration is determined by a number of reactivity insertions in addition to fuel compaction. The following appear to be the most important: (1) steel relocation from the core to the lower axial blanket, (2) spectrum-hardening-induced loss of rod worth, and (3) neutron reflection from the molten steel layer above and the solid steel layer below.

A new computer program called SCORIA (Slumped CORe Integrated Analysis) has aided in this event sequence evaluation. SCORIA is essentially a lumped heat capacity, thermal network analysis tool which includes conduction, forced convection, and radiation heat transfer from one node to another and accounts for the change of phase of steel and fuel. Currently, it solves the heat transfer problem in one dimension and has the capability to model many axial locations, although the axial components of conduction and radiation are neglected. SCORIA also includes a

model which parametrically accounts for the buildup of steel from the lower axial blanket blockage, the backfill of the assembly coolant channels by molten steel resulting in spillover into the interassembly spacing, and the blockage buildup in the interassembly spacing. A GCFR has been modeled in one dimension rod by rod including assembly walls from the center of the core through the radial blanket during an LOSC accident. The transient model begins at steady state, proceeds through circulator coastdown and reactor trip to the adiabatic core heatup, and culminates in complete core melting. Figure 3-4 is representative of the results on the core midplane. It shows the cladding, duct wall, and fuel melting radial progression across a GCFR core. Each explicitly denoted assembly (ASM-2, ASM-5, etc.) represents the hexagonal ring of assemblies in which it is found.

The results presented in Fig. 3-2 assumed that the helium circulators inertially coast down such that flow ceases in 230 s. The reactor is tripped 0.5 s after circulator power is lost. In contrast, if the accident occurs 1 week after shutdown, incipient cladding, assembly wall, and fuel melting would occur at 1050, 1600, and 2900 s, respectively.

As cladding and duct walls melt, molten steel is expectd to drip or flow by gravity toward the lower axial blanket. This process has been modeled as a film flow. In the absence of intra-assembly natural circulation, the molten steel cannot permanently resolidify in the core because the cladding melt front progresses eventually to the core bottom. The penetration of molten steel into the lower axial blanket and the buildup of a steel crust which blocks the coolant channels have been modeled. This calculation assumes conduction heat transfer from the flowing steel and an input temperature boundary condition at the fuel surface. The model is similar to the integral approach recommended by Epstein (Ref. 3-3). The major difference is that the current work models cladding as the "thermally thin" wall of a cylindrical tube. The model has been coded in a program called STEFINS. The results show that complete blockage of the coolant channel in the lower axial blanket and the spacing between

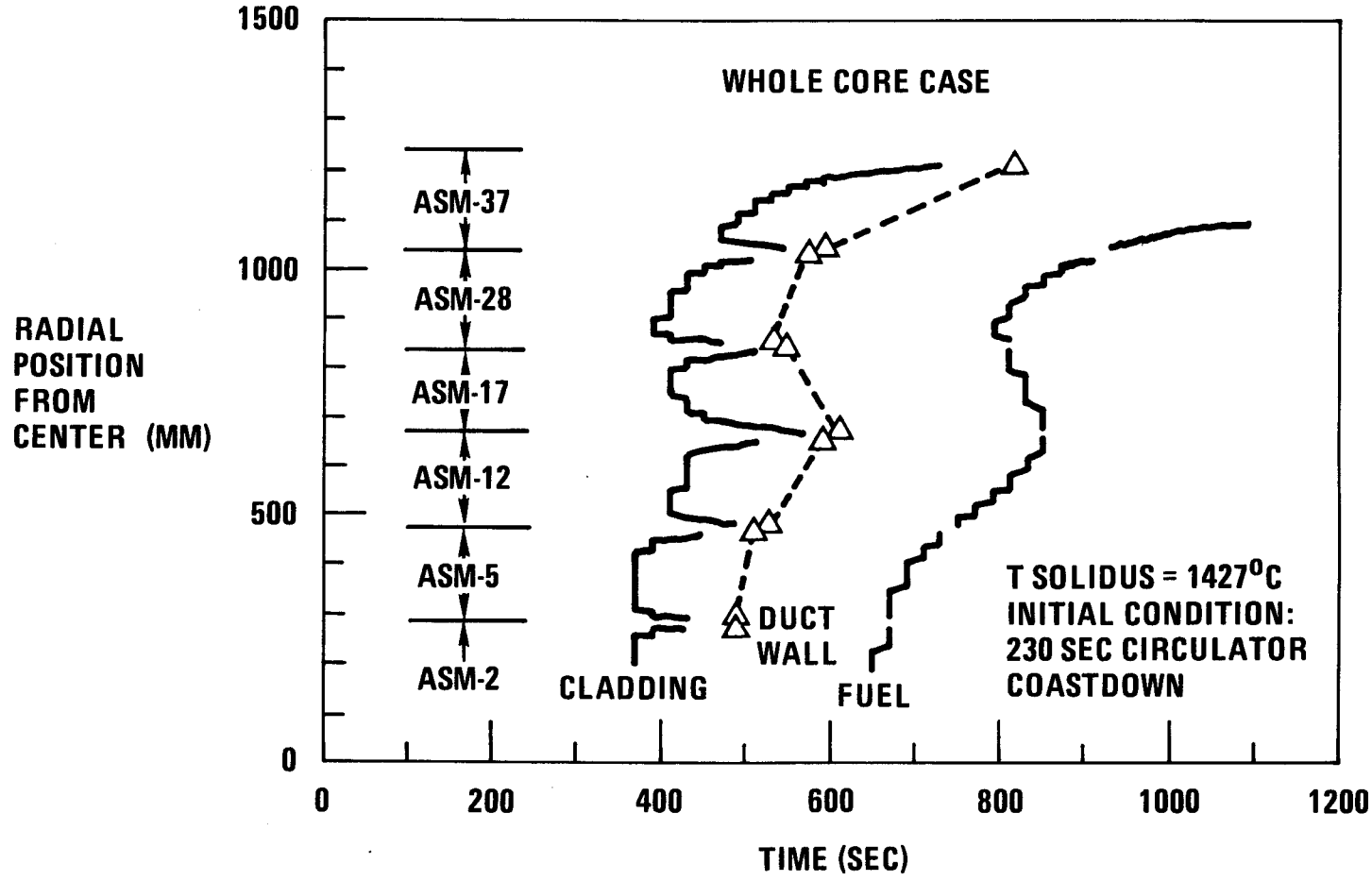

Fig. 3-4. Material melting sequence during an LOSC accident

assemblies is expected to occur within 50 mm below the core bottom. The rate of radial buildup of a solidified steel layer in the channel is between 2 and 5 mm/s.

3.3. RECRITICALITY PHASE

One postulated mode of fuel compaction which may induce recriticality is fuel melting and relocation onto the steel blockage. For purposes of analyzing this mode, one sequence of fuel relocation was assumed. It is not necessarily a mechanistic mode of fuel relocation. The melted portion of each fuel column was presumed to move downward to the steel blockage and displace its volume of molten steel, which in turn floated on the molten fuel. The upper still-solid portion of the fuel column was assumed to fall until it contacted the lower still-solid portion of the fuel column. Solid fuel column collapse was not considered in this sequence, and the upper axial blanket pellets were not allowed to fall. The result is to leave a neutronic void between the core fuel column and the upper axial blanket.

A timewise series of core material distributions was deduced from SCORIA by using the above fuel relocation assumptions. They were neutronically analyzed for the purpose of obtaining the fuel melt fraction, approximate time at criticality, and approximate ramp rate with an R-Z diffusion theory methodology which has been verified by transport theory (Ref. 3-4). The core was divided into six radial rings corresponding approximately to assembly rings and eight axial regions defined as follows:

Region	Description
1	Normal lower axial blanket
2	Lower axial blanket and/or core with steel plugged coolant channels
3	Steel blockage and molten fuel and remaining intact fuel columns

Region	Description
4	Molten fuel and duct wall and remaining intact fuel columns
5	Molten steel and duct wall and remaining intact fuel columns
6	Duct wall and remaining intact fuel columns and helium
7	Duct wall and helium
8	Normal upper axial blanket

The results are given below, and a schematic of the critical configuration is shown in Fig. 3-5:

Transient Time (s)	Configuration Detail	k_{eff}
0	Hot shutdown.	0.89
300	44% of cladding slumped. Top 77 mm of lower axial blanket plugged.	0.91
770	6.6% of fuel molten. Nearly all cladding slumped. Some duct wall melting.	0.92
770	Same with no fuel spreading between assemblies.	0.94
870	21% of fuel molten. Most of assembly walls melted. Molten fuel in every assembly.	0.93
970*	31% of fuel molten. All but outermost assembly wall slumped.	0.99
1110	45% of fuel molten.	1.09

*Figure 3-5 is the configuration at this time.

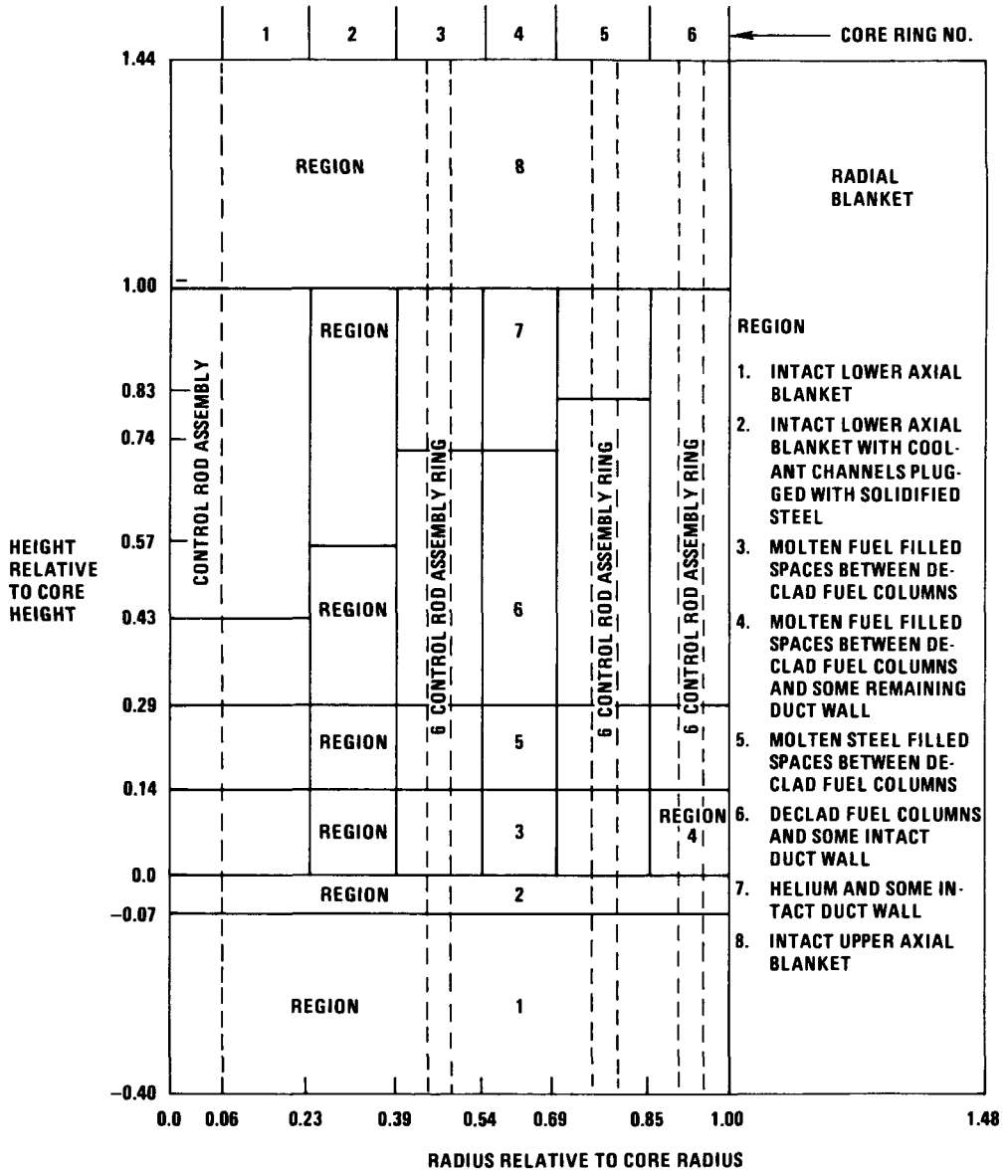

Fig. 3-5. LOSC critical core configuration

At criticality the reactivity ramp rate is 17¢/s. This represents the ramp rate which is attained by decay heat alone. As the core nears critical, some faster melting rate would be expected because of the onset of significant fission heating. All cases but the fourth assumed that the molten fuel could spill from one assembly with a higher fuel elevation to another with a lower elevation. Comparison of the third and fourth cases (both with 6.6% of fuel molten) shows the large sensitivity in the results to a radial fuel spreading assumption. In the fourth case, fuel was constrained so that it stayed in its own assembly. Prohibiting spreading increased the reactivity for this case by about $5. It may be possible for criticality to be calculated from molten fuel slumping of the interior 26 assemblies alone if fuel is not assumed to spread.

Another mode of fuel relocation which may induce a criticality is the crumbling and compacting of fuel columns. Calculations using the same methodology have been performed to determine the packing of fuel fragments required for criticality if an entire core should crumble. These model a core which has all control rods fully inserted, all cladding and assembly wall steel layered up from the core bottom, and all the core fuel (which is still solid) crumbled into this steel layer. Molten cladding has filled the spaces between the crumbled fuel fragments. The results are shown in Fig. 3-6. It was found that this configuration is critical if the non-fuel fraction in the fuel region is less than 60%. The reactivity addition rate is about $1.40 per percent of fuel packing fraction increase. Another perspective is that criticality would occur if the top 28% of all fuel columns crumbled and filled the coolant channels above the lower axial blanket at the pellet density.

3.4. TRANSITION PHASE

An LOSC could result in a mild neutronic burst or gradual melting, either of which could lead to multiple recriticalities. This phase of a CDA is called the transition phase. The analysis done for the upflow/-downflow core study does not consider the transition phase. Calculations were performed up to the first criticality only.

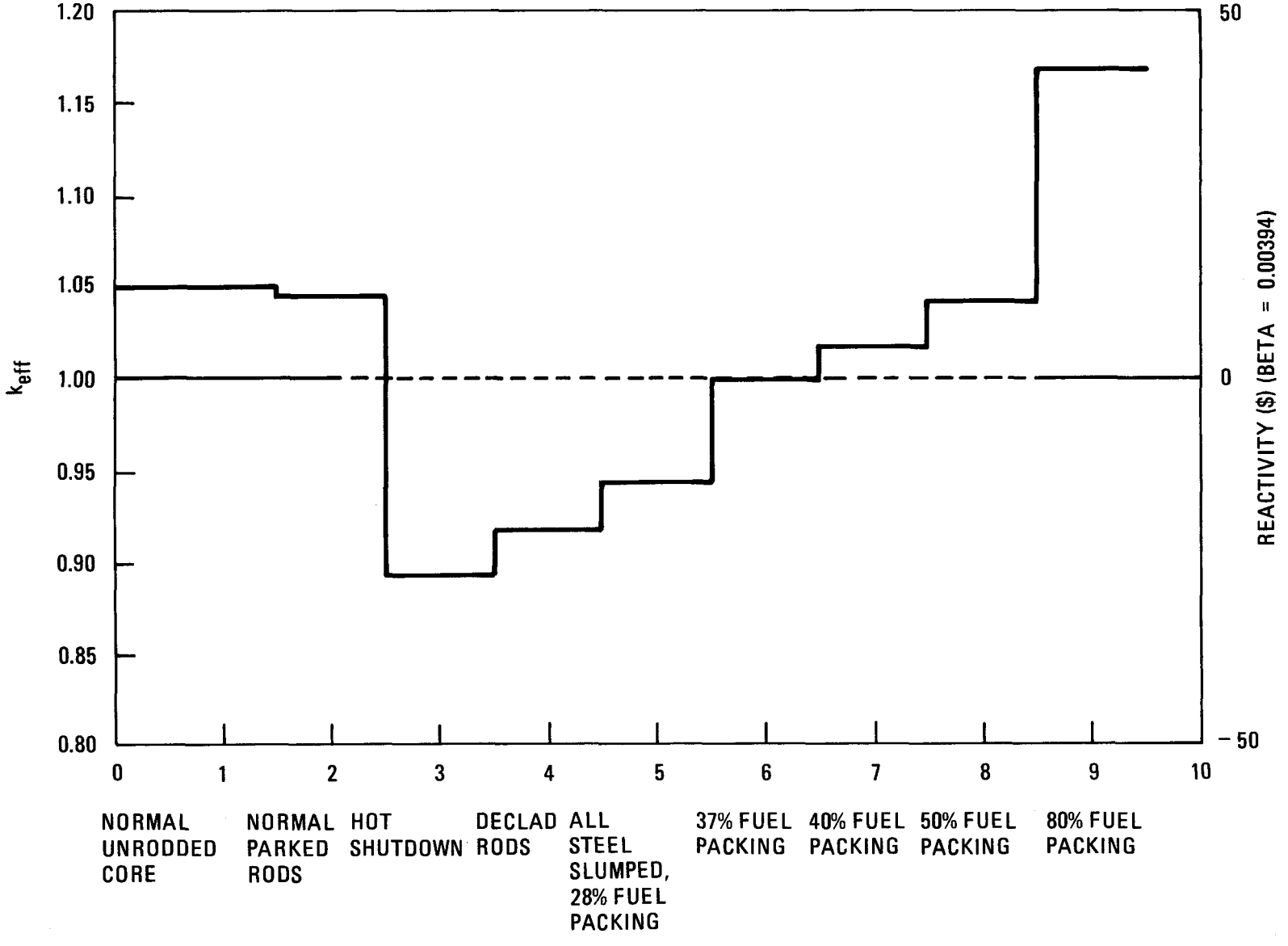

Fig. 3-6. Crumbled core reactivity potential

The analysis of the transition phase of a CDA is very complex. Little is known about the accident progression and the basic mechanisms involved. Four key phenomena are associated with the transition phase: recriticality, fuel removal mechanisms, hydrodynamics, and heat transfer. The transition phase deals with the accident from total core melt (or recriticality) to a subcritical, coolable state. Multiple criticalities are the major concern in transition phase analysis attempts to answer two difficult questions: (1) Are multiple bursts possible?; (2) What are their results?

If it can be shown that recriticality is impossible, it is only necessary to design the PCRV to contain the molten fuel. Three arguments used to demonstrate no-recriticality are extensive fuel removal from the core, poison solution in the fuel, and a boiled-up core. Since the GCFR core is pressurized, it will not be in a boiled-up state. Therefore, no-recriticality can be based only on fuel removal or solution poisoning.

The main mechanism for fuel removal from the core is the flowing of fuel in a channel (axial blankets). Several models have been developed to assess the penetration depth of fuel in blankets, but a better understanding of fuel/steel conditions is needed.

The effect of fuel dispersal by disassembly can be evaluated by use of the VENUS-II computer code (Ref. 3-5). Before this code can be used, a better understanding of the precriticality phase is needed.

Two-phase fuel hydrodynamics is not as important for GCFR safety as liquid metal fast breeder reactor (LMFBR) safety. The slumped fuel will be a non-boiling state except during a fission pulse. The main area of hydrodynamic research for the GCFR is fuel response to a mild recriticality. In this case there is a need to couple neutronics and fuel motion. The application of codes such as FX2-POOL (Ref. 3-6) or SIMMER-II (Ref. 3-7) is a technique available for hydrodynamic analysis.

Molten fuel heat transfer is important for GCFR analysis. Better correlations are needed for a wide variety of accident conditions. A bulk heat transfer model [such as Baker's model (Ref. 3-8)] could be used in addition to FX2-POOL or SIMMER-II for detailed analysis. Comparisons could be made between SIMMER-II and bulk flow models.

3.5. PAFC PHASE

3.5.1. In-Vessel PAFC Analyses

For the downflow design, failure of two out of three CACS loops results in core melting. The remaining loop may be available for PAFC cooling. A separately designed natural helium convection cooling system may also be available for PAFC cooling. It was assumed that helium cooling is always available in a downflow design.

For the upflow design, failure of forced flow in all three CACS loops does not result in core melting. Degradation of natural circulation would also be needed for core melting. Since the degree of natural circulation degradation necessary for core melting was not known at the time of the analysis, it was desirable to determine whether the long-term PAFC is successful with only cavity liner cooling. For this reason, it was assumed that natural convection is not available for PAFC cooling in the upflow concept. Continued work on natural circulation will quantify the degradation which can be factored into future analysis.

3.5.2. Upflow Core Meltdown Conditions

The volume of molten materials following a core meltdown in an upflow GCFR depends upon the failure modes of the core support plate. The time the core support plate fails depends upon the location of the core materials relative to the core support plate.

The earliest failure of the core support plate may be when molten fuel and molten steel refreeze inside the grid plate coolant channels.

Under this condition, one-third of the fuel and cladding may be contained within the grid plate. By adiabatic heating, the average temperature of the grid plate reaches the failure limit (assumed 1100°C) 3 hr after the accident.

If molten fuel and steel do not refreeze in the grid plate, they will relocate to the PCRV floor, forming a debris pool. The molten pool is assumed to maintain the melting temperature of steel (1427°C) until all the steel from the MFCS and the core structure melts. The lower surface of the core support plate would be exposed to the hot debris. A radiation heat transfer model was used to calculate the transient heating of the core support plate. The remaining core, the upper and lower plenum, and the cavity liner cooling system were included in the model (Fig. 3-7). The volatile fission products were assumed to remain in the reactor cavity uniformly distributed in helium. Figure 3-7 shows the transient heating of the core support plate for three locations. The midplane location reaches the 1100°C failure limit about 9 hr after the accident.

It was determined that the core support plate would fail between 3 to 9 hr after a core meltdown.

3.5.3. Analysis of Upflow Core PAFC

A two-dimensional heat transfer model was developed for PAFC analysis following the core meltdown phase. The following major assumptions were made in the analysis:

1. Only materials from the center portion of the core barrel drop to the MFCS after the failure of the core support plate. The outer rim of the grid plate (outside the radial blanket) and shielding assemblies remain in place.

2. Owing to the uncertainties in the mode of core meltdown, the transient model begins at the time of accident initiation instead of the failure time of the core support plate.

3. The debris mass forms three layers. Steel from the core region and the MFCS forms a layer on top of the fuel and blanket materials. Shielding materials form the uppermost layer.

4. Only the cavity liner cooling system removes the post-accident decay heat. There is no helium convection cooling to the heat exchangers.

The MFCS was designed to contain only the amount of core debris stated in Assumption 1. Subsequent failure of the remaining grid plate, the hanging shield, and the outer radial shield may cause a fuel spillover into the side cavities because of the low duct location in an upflow design. The purpose of this analysis was to determine whether the subsequent heating in the PAFC phase would indeed cause the remaining reactor internal structures to fail.

Results of the transient analysis are shown in Figs. 3-8 through 3-11. Figure 3-8 shows the melting and refreezing of the fuel and steel debris. The fuel and steel pools both start without a lower crust. The lower fuel crust develops rapidly and later exceeds the upper and sideward fuel crusts. This is because, in the fuel pool, the convection-dominated heat transfer model always predicts that a smaller fraction of the heat removal is downward rather than sideward and upward. The fuel pool reaches a maximum size of 6 m^3 (65% of the fuel plus blanket materials) in 15 hr. A lower steel crust does not develop in the 100-hr time span of the analysis. From 20 to 53 hr, the steel region is completely molten. Then the sideward crust regrows and a general cooling process of the steel region begins.

Figure 3-9 shows temperature transients of cavity internal structures. The temperature of the remaining core support plate reaches 1100°C (the assumed failure limit) at 41 hr after the accident. A maximum temperature of 1135°C would be reached at 64 hr. The lower portion of the radial shield reaches a maximum temperature of 1090°C at 51 hr. Other

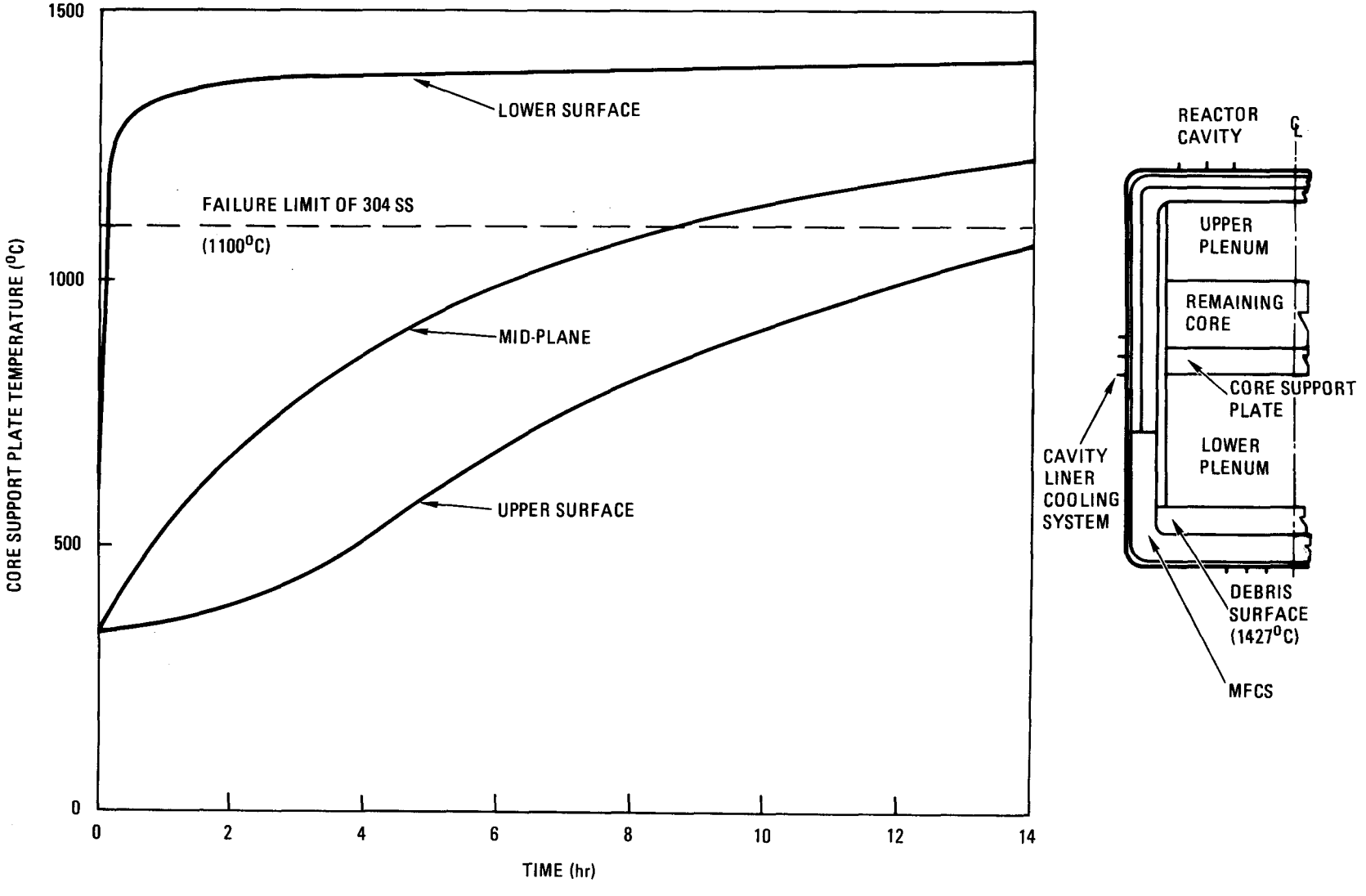

Fig. 3-7. Core support plate temperatures at three locations

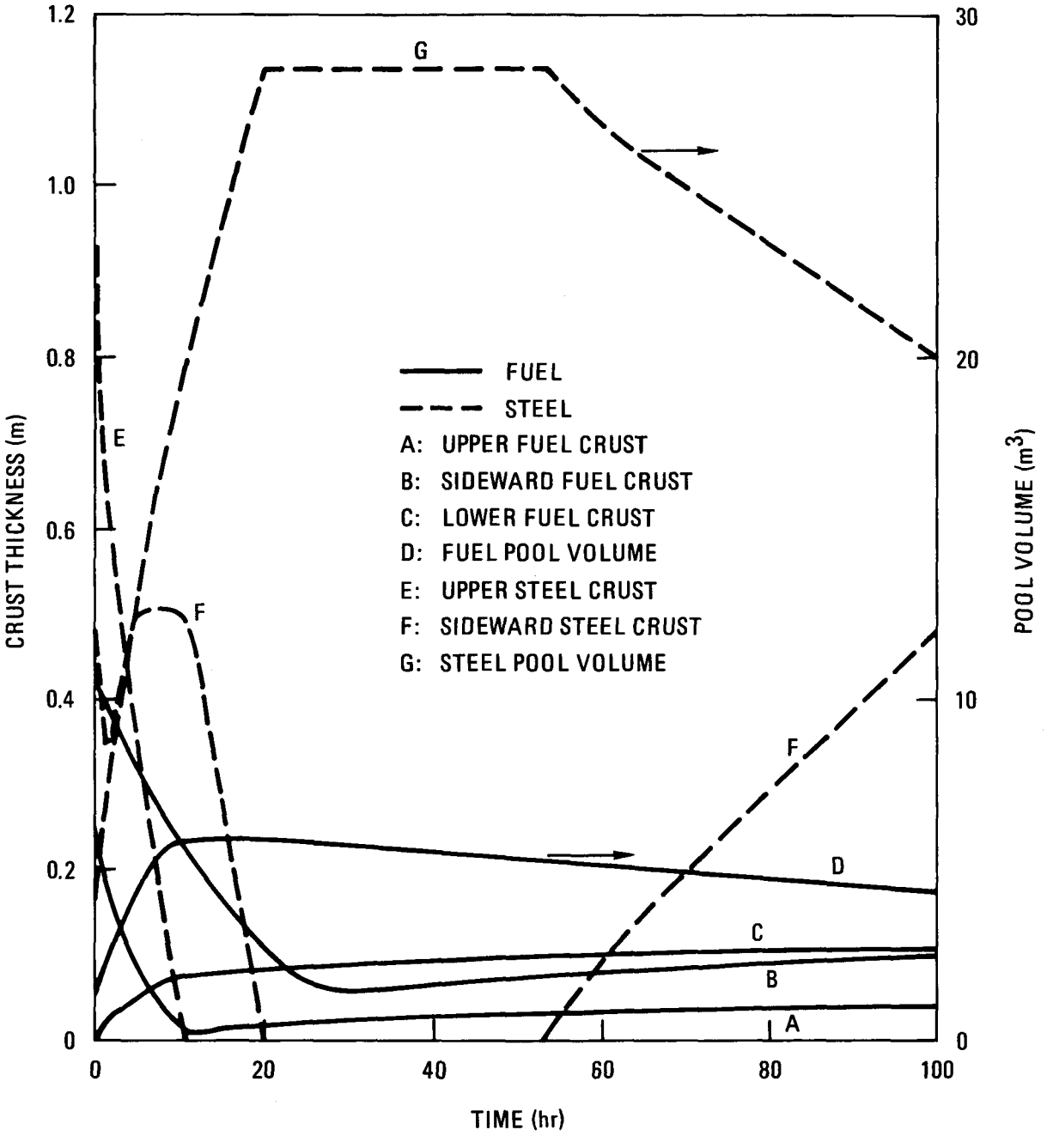

Fig. 3-8. Crust thickness and pool volume of fuel and steel

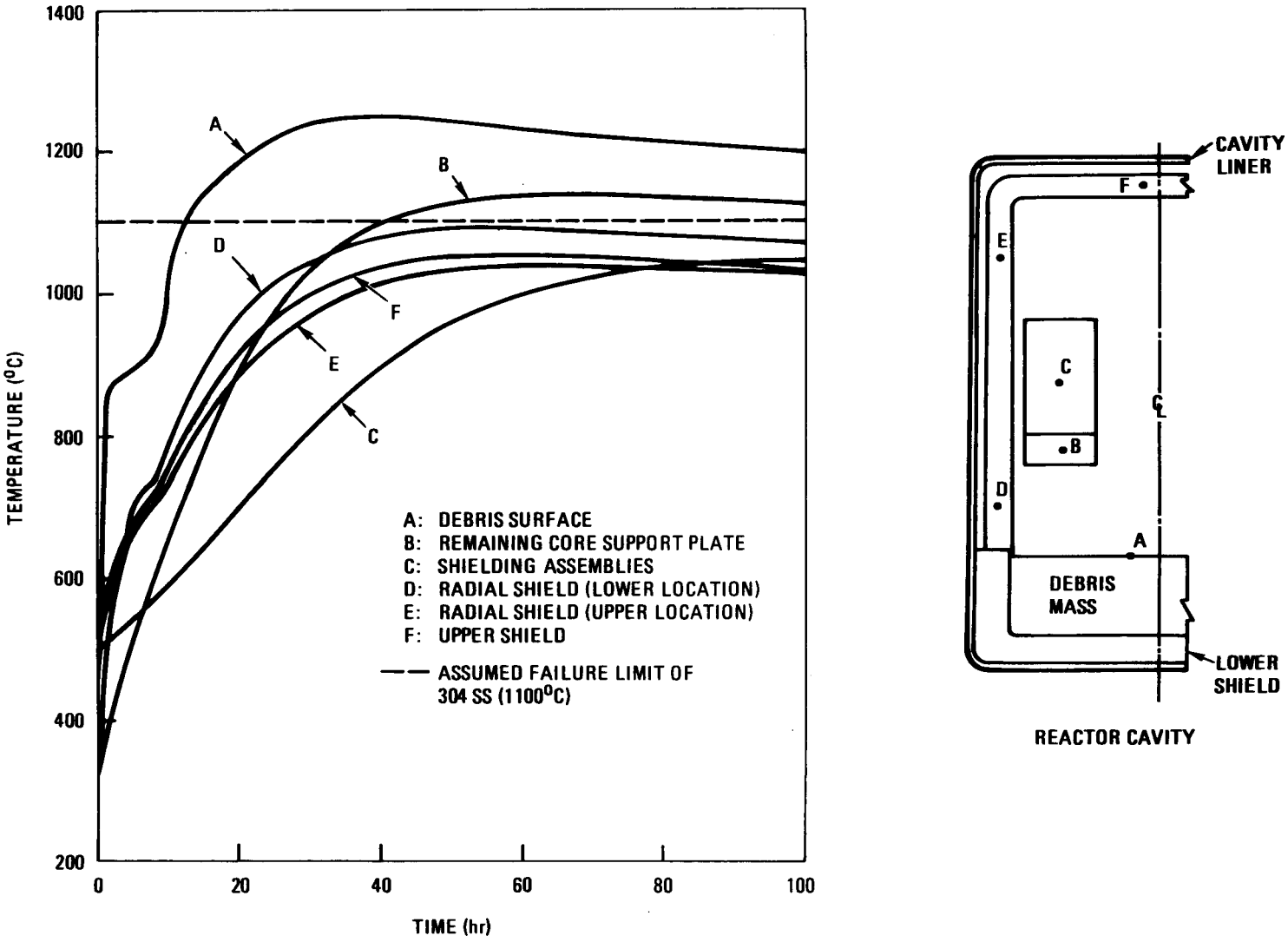

Fig. 3-9. Temperature history of reactor internal structures

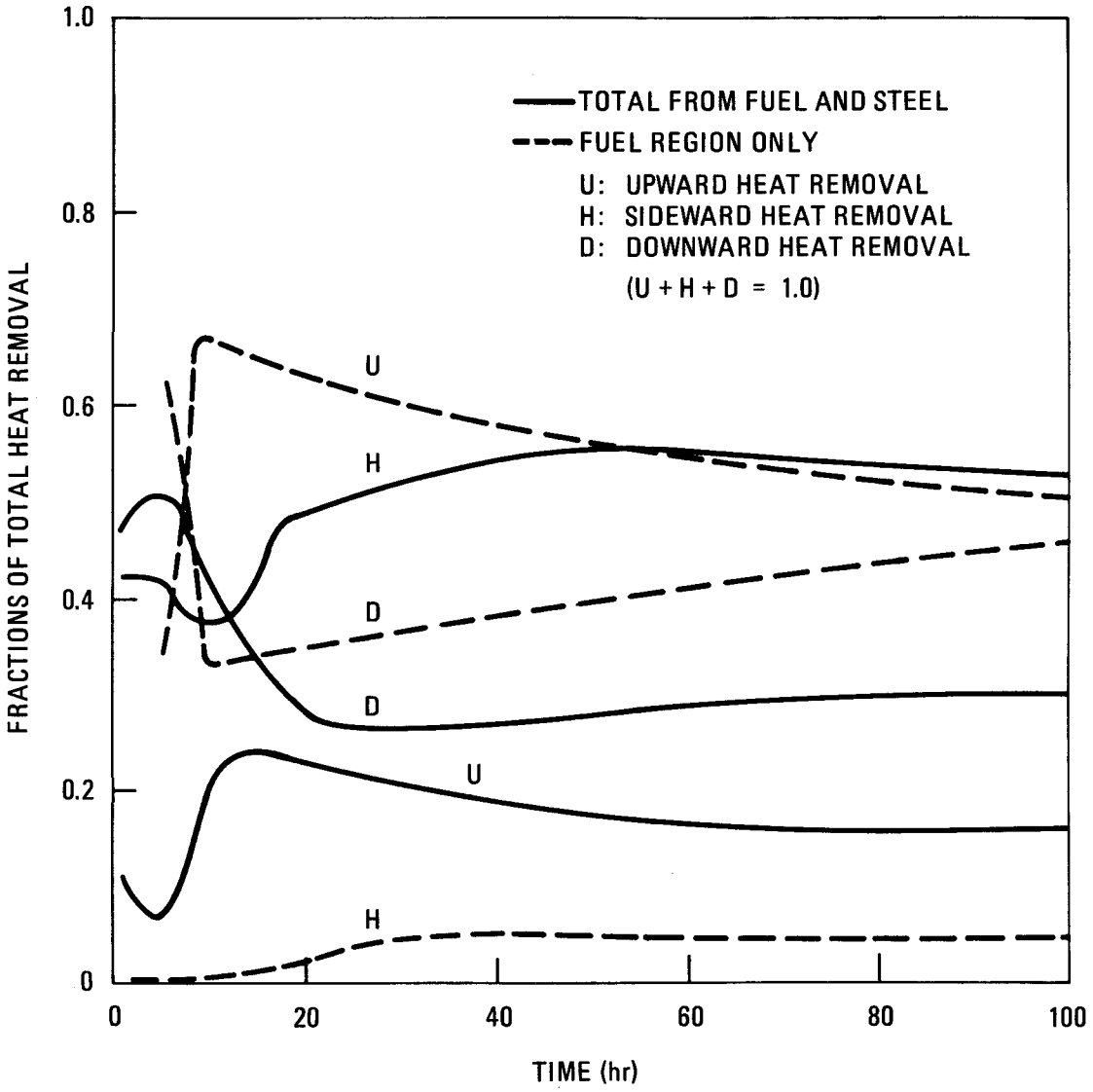

Fig. 3-10. Distribution of directional heat removal from debris mass

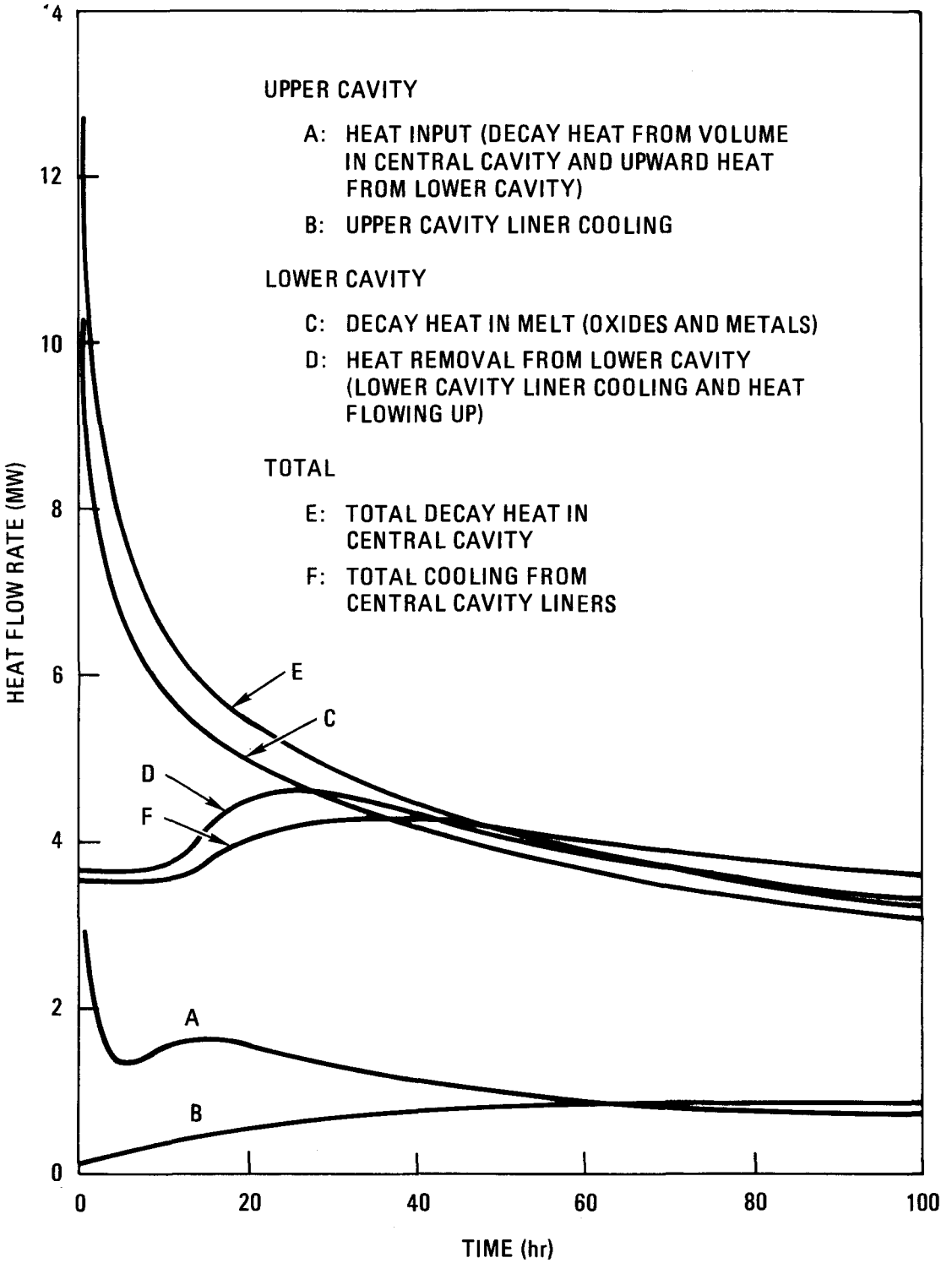

Fig. 3-11. Heat balance in central reactor cavity

locations of the radial shield reach somewhat lower maximum temperatures. The shielding assemblies heat up slowly even beyond 100 hr, owing to their large heat capacity and void spaces, but will not exceed the temperature of the remaining core support plate.

Figure 3-10 shows the distribution of directional heat removal from fuel and steel debris. In the fuel region only, the upward heat removal is calculated to be greater than 50% of the total heat removed for up to 100 hr and the sideward heat removal is insignificant. However, the sideward heat removal is calculated to be dominant for the combined fuel and steel core debris. The upward heat removal reaches only 25% of the total and decreases below 20% after 40 hr. The large fraction of upward heat removal from the fuel pool is redirected to the side wall of the steel pool. Therefore, the combined upward heat removal is greatly reduced.

Figure 3-11 shows the heat balance. In the lower cavity, a quasi-steady state is reached 28 hr after the accident, while in the upper cavity, 65 hr is required to reach the quasi-steady state. These curves also show that heat flow to the cavity liner above the MFCS on the PCRV floor is less than 1 MW and the total decay heat burden to the cavity liner is less than 5 MW. The cavity liner cooling capacity is 2.5 MW during normal operation. Therefore, only a two-fold increase of the liner cooling heat exchanger capacity will satisfy the PAFC cooling requirement.

Parametric studies show that with 25% reduction of upper cavity insulation, the reactor internals can be maintained below 1100°C, the assumed failure limit (Table 3-1). Depressurization of the system to equilibrium pressure with the containment gives even greater temperature margin below the failure limit (Fig. 3-12) because most of the volatile fission products are removed from the PCRV. Without any water or helium cooling, the cavity liner of the lower reactor cavity fails 6 hr after core meltdown; but the fuel temperature remains well below its boiling point within the 6 hr (Table 3-2). Under PAFC conditions, a greater temperature margin below the structural failure limit can be provided by

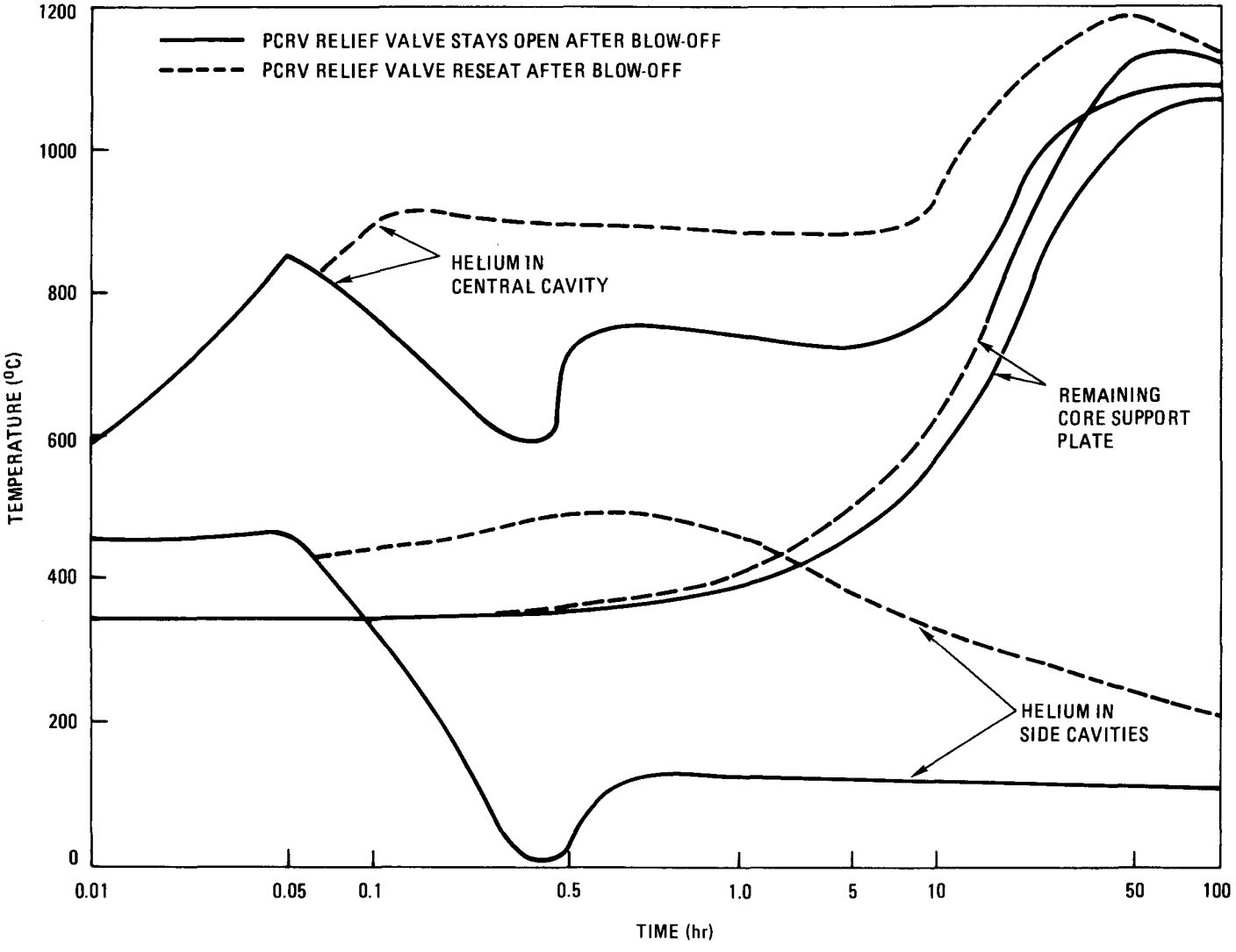

Fig. 3-12. Effect of PCRV relief valve opening on reactor internal temperatures

TABLE 3-1
EFFECT OF CAVITY LINER INSULATION THICKNESS

	Thermal Barrier Thickness	
	Case I (0.1 m)	Case II (0.076 m)
Maximum temperature of remaining core support plate, °C	1135	1100
Maximum temperature of radial shield, °C	1090	1050
Maximum temperature of debris surface, °C	1244	1223
Maximum temperature of upper cavity liner, °C	93	95
Maximum heat removal from upper cavity, MW	0.84	0.96
Maximum heat flux of upper cavity liner, kW/m^2	3.7	4.2
Fraction of upward heat removal from lower cavity at 50 hr	0.17	0.19
Fraction of sideward heat removal from lower cavity at 50 hr	0.56	0.54

TABLE 3-2
CAVITY AND DEBRIS TEMPERATURES UNDER NO LINER COOLING CONDITION

Parameter	Time (hr)					
	2	3	4	5	6	7
Temperature of bottom cavity liner, °C	724	938	1141	1333	1522	1699
Temperature of sideward (lower) cavity liner, °C	328	372	407	438	466	492
Temperature of remaining core support plate, °C	396	419	440	460	480	498
Temperature of radial shield (lower location), °C	501	542	571	594	612	628
Temperature of fuel pool, °C	2922	2921	2921	2920	2920	2921
Temperature of steel pool, °C	1446	1445	1444	1444	1445	1469
Helium temperature in central cavity, °C	779	761	768	773	778	789
Pressure inside PCRV, MPa	9.7	8.7	8.9	9.1	9.2	9.3

several design modifications. These modifications include a thinner thermal barrier, an automatic depressurization system, and an enlarged lower cavity with increased amount of sacrificial materials. Therefore, a PAFC system using cavity liner cooling alone but with sufficient failure margin provided by the design may be feasible.

3.5.4. MFCS Containment Volume Estimates and Spillover Evaluation

The core debris volumes were calculated for different meltdown conditions to determine the potential for spillover into the PCRV side cavities from the MFCS. Three cases of meltdown were investigated. In Case I, all regions containing fuel were assumed to fall to the PCRV bottom along with supporting materials. For the downflow design, the core and blankets fall. The tops of the fuel pins and outlet nozzles also fall into the MFCS. Failure of the grid plate in the upflow design results in all of the fuel and blanket assemblies falling into the MFCS. Since it would be difficult to show that refueled regions would not melt or otherwise fail during a core disruptive accident, Case I represents the minimum volume allowable for the MFCS. It is the base case.

Once the fueled sections drain into the MFCS, additional materials may fail owing to radiation heating from the molten debris. Case II represents the additional material failing from radiative overheating. This includes the lower or hanging shields and the radial shield assemblies. It also includes some remaining portions of the fuel and blanket assemblies in the downflow concept.

If heating by radiation continues long enough, the radial shield could also fail. Case III includes the radial shields in addition to the accumulated inventory of Cases I and II.

The results of the volume calculations are shown in Table 3-3 for the downflow and upflow cores. The minimum containment volumes required (Case I) for MFCSs are 13 m^3 for the downflow core and 27 m^3 for the upflow core.

TABLE 3-3
CORE DEBRIS VOLUME (m^3) VERSUS EXTENT OF MELTDOWN

	Steel	Fuel and Blanket	Shield	Control	Total
Case I					
Downflow core	3.841	8.799	0.169	0.072	12.881
Upflow core	13.161	9.102	4.091	0.091	26.445
Case II					
Downflow core	41.605	8.799	71.341	0.072	121.817
Upflow core	25.143	9.102	20.649	0.091	54.985
Case III					
Downflow core	83.212	8.799	174.734	0.072	268.817
Upflow core	54.340	9.102	80.910	0.091	144.443

A scoping analysis was performed for the upflow core design to determine the consequences of fuel spillover into side cavities following a core meltdown accident. Molten materials will not overflow the MFCS until radial shields fall from their support about 120 hr after the accident begins. A homogeneous mixture of fuel and steel was assumed to flow equally into the six side cavities.

The two major consequences of fuel spillover are PCRV failure from melt-through and hydrogen production from water ingress. The spilled-over molten debris was calculated to penetrate through the bottom of the steam generator cavities about 20 hr after spillover and through the bottom of the auxiliary heat exchanger cavities about 12 hr after spillover. Thermal radiation may cause melting of the steam generator inlet tubes but not the core auxiliary heat exchanger tubes. Therefore, water may potentially enter the cavity and react with the molten steel and graphite debris spilled from the core cavity. If all of the steam generator inventory in all three loops is assumed to react with the steel and graphite, then the quantity of hydrogen potentially produced is about 1% of the quantity of oxygen (from air) in the containment.

3.5.5. Ex-Vessel PAFC Analyses

Analyses were performed to evaluate the integrity of the PCRV lower head following cavity liner melt-through by molten fuel in the absence of both an in-vessel MFCS and all liner cooling. Several possible failure modes of the PCRV lower head have been identified. They can be grouped into two categories: (1) gross pool growth into concrete and (2) localized attack on the refueling penetration. The first category applies equally to an upflow or a downflow core, while the second applies only to a downflow core.

3.5.5.1. Gross Pool Growth Into Concrete. If a 50,000-kg molten core mass is postulated to fall upon the lower PCRV cavity liner, and all liner coolant flow has stopped, then the molten mass will penetrate the cavity

liner 6 hr later. This time assumes complete spreading across the central cavity diameter, equal heat fluxes in all directions (Ref. 3-8), and a constant liquid/solid interface temperature at the liner of 1400°C.

Based on the decay heat rate at 6 hr, i.e., 6.5 MW in the fuel melt, the initial heat flux at the pool boundaries was 105 kW/m^2. The initial temperature of the concrete was 49°C. Using the data for Clinch River Breeder Reactor (CRBR) concrete (Ref. 3-9), the total heat required to raise the concrete temperature from 49°C to the melting point (including heat contributed to water vapor release and concrete decomposition) was 3.55×10^6 J/kg. Assuming 6 wt % water in CRBR concrete, the steel-water reaction heat during pool growth was 9×10^4 J/kg. Using 2370 kg/m^3 as the density of CRBR concrete, the initial pool growth rate was 44 mm/hr. The actual pool growth rate is a decreasing function of time, however, owing to the increasing pool surface area, the decreasing decay heat rate, and pool growth. To avoid a complicated pool growth calculation, a curve fit to the superficial gas velocity (Ref. 3-10) (which is proportional to the linear pool growth rate) was employed, which gives

$$\text{pool growth rate} = 136\ t^{-0.63}\ (\text{mm/hr}) \quad , \tag{3-1}$$

where t is time in hours after shutdown. Integration of Eq. 3-1 with respect to time from time = 6 to t gives the linear pool growth (L) as

$$L = 0.37\ t^{0.37} - 0.72\ (\text{m}) \quad . \tag{3-2}$$

The time t to accumulate a pool growth L can be expressed by

$$t = \left(\frac{L + 0.72}{0.37}\right)^{2.7}\ (\text{hr}) \quad . \tag{3-3}$$

The PCRV lower head, with a single refueling penetration, has a thickness of 4.33 m. The first row of axial PCRV tendons is located radially 0.6 m away from the cavity liner. Therefore, using Eq. 3-3, melt-through of the 4.33-m lower head would take 48 days. If it is assumed

that the lower head would fail when one-half of the concrete (2.17 m) had melted, melt-through would still take 256 hr. The first row of tendons could be reached by sideward pool growth in 31 hr. Therefore, it appears that the PCRV lower head failure due to loss of tendons under full system pressure would occur much earlier than the failure due to a gross pool growth in the downward direction.

3.5.5.2. Localized Attack on Refueling Penetration. For the downflow core design, molten fuel can enter into the annular gap between the refueling plug and the PCRV liner. Molten fuel can heat the surroundings of the plug, causing the plug structure resting on the locking ring to fail. In this very unlikely event, the plug would either drop out under gravity or be accelerated by the helium pressure inside the PCRV.

A refueling penetration design from Ref. 3-11 was chosen for the analysis. The bottom portion of the PCRV lower head with refueling plug is shown in Fig. 3-13. The top shoulder was assumed to melt immediately upon contact by penetrating molten fuel, so the fuel was assumed to penetrate to the lower shoulder near the bottom of the plug. A gap size of 6.35 mm was assumed. To maximize the heat source, molten fuel from only the active core and axial blankets was modeled. Transient analyses began 30 min after the accident.

The temperatures of fuel, steel, and PCRV concrete at the key locations were obtained from transient analyses. The fuel temperature exhibits a sharp decrease initially, then slowly rises to a maximum of 1100°C at about 200 hr. The maximum temperatures of all steel components (including the PCRV liner, the lower shoulder, the locking ring, and the O-ring seal) are well below the failure temperature of 1100°C for 200 hr. Problems remain with the PCRV concrete temperatures, which rise beyond the possible 540°C failure limit. Concrete temperatures reach 540°C near the fuel region and the locking ring in 40 and 80 hr, respectively. Therefore, beyond 40 hr, a potential may exist for failure of PCRV concrete. Table 3-4 compares the PCRV concrete failure times from different failure

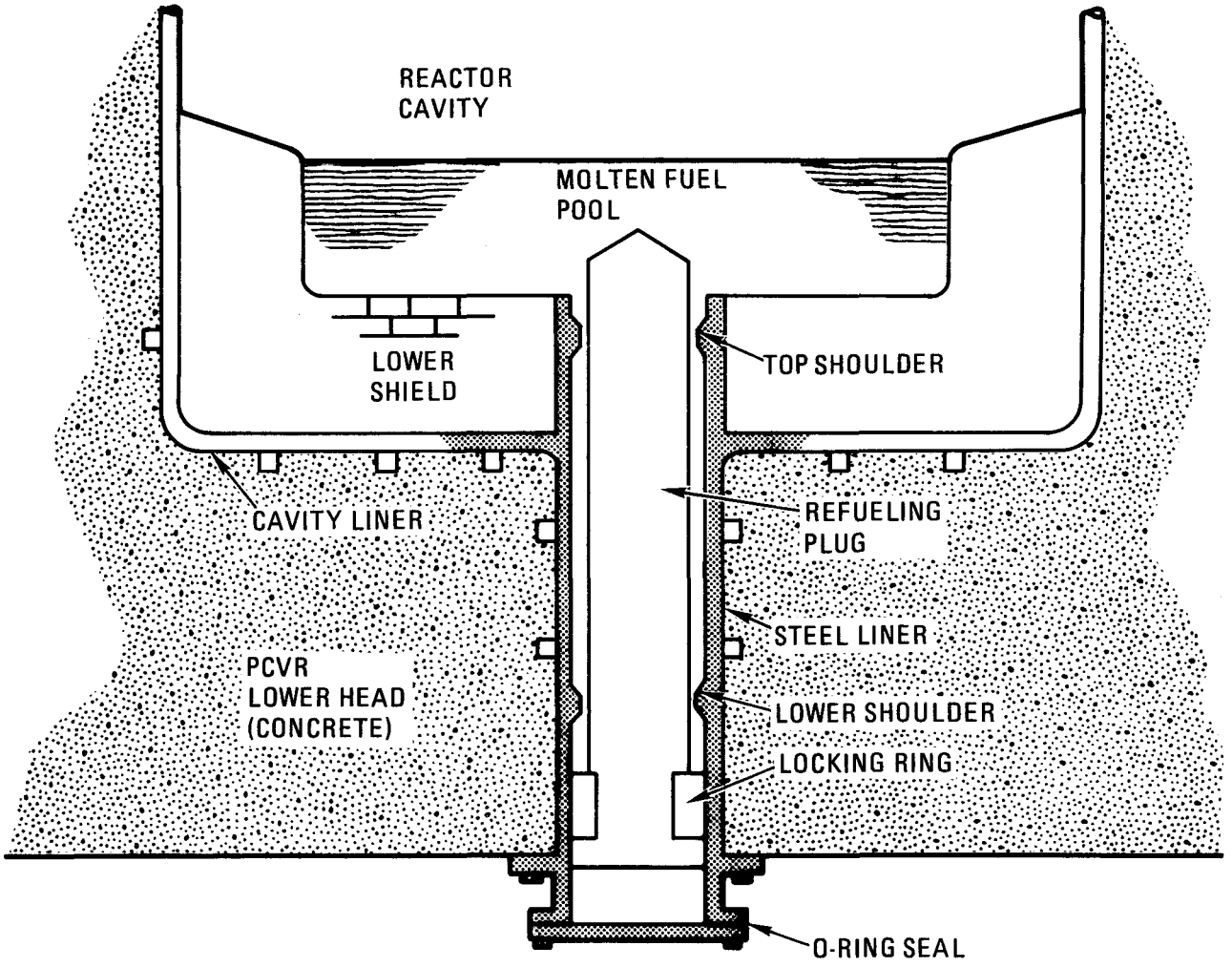

Fig. 3-13. PCRV lower head and refueling penetration

TABLE 3-4
COMPARISON OF POSTULATED PCRV FAILURE MODES

Cause of PCRV Failure	Time of Failure (After Accident Initiation) (hr)	Applicable to Upflow or Downflow Core
Failure of first row of PCRV tendons	31	UF and DF
Failure of PCRV concrete (near fuel in refueling gap)	40	DF
Failure of PCRV concrete (near locking ring of refueling plug)	80	DF
Failure of lower shoulder of refueling plug	> 200	DF
Failure of locking ring of refueling plug	> 200	DF
Failure of PCRV lower head by melting of one-half of concrete	256	UF and DF
Failure of PCRV lower head by melting of full concrete thickness	1150	UF and DF

modes. The postulated scenario leading to the failure of PCRV tendons presents the earliest threat to the integrity of the PCRV lower head for both the upflow and downflow designs.

REFERENCES

3-1. Torri, A., and J. L. Tomkins, "Accident Termination by Element Dropout in the GCFR," Proceedings of the Fast Reactor Safety Meeting, Chicago, October 1976, pp. 1183-1194.

3-2. Properties for LMFBR Safety Analysis, Argonne National Laboratory, April 1976 (ANL-CEN-RSD-76-1).

3-3. Epstein, M., "The Growth and Decay of a Frozen Layer in Forced Flow," Int. J. Heat Mass Trans. 19, 1281-1288 (1976).

3-4. "Gas-Cooled Fast Breeder Reactor, Quarterly Progress Report for the Period November 1, 1978 through January 31, 1979," DOE Report GA-A15237, General Atomic Company, February 1979, pp. 7-1 through 7-11.

3-5. Jackson, J. F., and R. B. Nicholson, "VENUS-II: An LMFBR Disassembly Program," USAEC Report ANL-7951, Argonne National Laboratory, 1972.

3-6. Abramson, P. B., "POOL - A Two-Dimensional Three-Component Coupled Hydrodynamic Thermodynamic Computer Model for Boiling Pools of Fuel and Steel," Argonne National Laboratory, RSA-TM-3, 1975.

3-7. Smith, L. L., "SIMMER-II: A Computer Program for LMFBR Disrupted Core Analysis," Los Alamos Scientific Laboratory Report NUREG/CR-0453, 1978.

3-8. Baker, L., et al., "Heat Removal from Molten Fuel Pools," Proceedings of the International Meeting on Fast Reactor Safety and Related Physics, October 5-8, 1976, Chicago, Illinois, p. 2056 (CONF-761001).

3-9. "Reactor Development Program Progress Report," DOE Report ANL-RDP-62, Argonne National Laboratory, July-August 1977, p. 6-46.

3-10. Baker, L., et al., "Core Debris Penetration into Concrete," Proceedings of the Third PAHR Information Exchange, Argonne, Illinois, Argonne National Laboratory, p. 223 (ANL-78-10).

3-11. "Gas-Cooled Fast Reactor Utility Program Progress Report for the Period January 1, 1971 through June 30, 1971," General Atomic Company, unpublished data.

4. COMPARISON OF UPFLOW VERSUS DOWNFLOW GCFR FOR CORE DISRUPTIVE ACCIDENTS

4.1. LOSC ACCIDENT MITIGATION

4.1.1. Introduction

The potential for recriticality was demonstrated in the previous section. A recriticality would, of course, create the potential for substantial fuel mobilization and dispersal. It would then be appropriate to consider possible approaches for preventing recriticality and containing the mobilized fuel. The following five levels of investigation could be pursued as a general LOSC consequence minimization approach:

1. Prevent cladding melting either by natural convection in helium for pressurized conditions or by natural convection in a water-flooded PCRV for depressurized conditions.

2. Prevent recriticality by (a) timely addition of sufficient neutron absorber material (poison), (b) timely drainage of molten fuel and steel, or (c) individual or small group assembly fallaway (downflow core only).

3. Minimize the fuel vapor fraction and work potential. This level requires investigation of the accident transition phase.

4. Contain the accident-generated energy within the PCRV and minimize fuel vapor exterior to the PCRV. This level would require a molten core retention system and various aerosol depletion devices such as sprays, filters, recirculation systems, and/or blowdown tanks.

5. Contain the accident-generated energy within the PCRV and minimize fuel vapor exterior to the containment/confinement buildings. This level would depend on depletion of fuel aerosols assisted by containment sprays, filters, and recirculation systems.

The major distinctions between an upflow and a downflow core are found in the potential for natural convection in helium (level 1) and in the recriticality prevention mechanism of duct fallaway (level 2). If either level 1 or 2 is successful, then level 3 would not be required for LOSC accident mitigation. Levels 4 and 5 may be unavoidable for either core. Since natural convection is treated elsewhere, this section focuses on level 2, recriticality prevention by poisoning, drainage, and fallaway.

The success or failure of potential mitigating features in the two concepts (upflow or downflow) depends upon the phenomenological timing of material removal versus recriticality. Figure 3-2 summarizes the timing of major events. During the cladding relocation phase, single assembly fallaway may begin in the downflow core. Drainage of molten steel and fuel through designed drainage paths and timely addition of sufficient neutron absorber material are potential recriticality prevention features in either concept.

It is apparent that recriticality may be prevented during an LOSC in the upflow (or downflow) core by sufficient addition of poison material. In order to investigate the feasibility of this approach, three activities were required: (1) Select the appropriate absorber material; (2) determine the amount of poison required to keep a slumped core subcritical; and (3) determine the design feasibility of keeping the poison available and inserting it when required.

The criteria for selecting an absorber material for recriticality prevention in a molten slumped core are as follows:

1. A melting temperature slightly below that of UO_2 and substantially above that of stainless steel.

2. Solubility of the liquid in molten UO_2.

3. Density similar to that of UO_2.

4. Sufficiently fast solubility rate.

5. Maximization of the fast spectrum neutron absorption cross section.

Criteria 2 and 3 eliminate B_4C as a candidate. Criteria 1 through 4 are satisfied by rare earth oxides. They have melting points in the 2200° to 2400°C range. At the UO_2 melting temperature, their heats of solution are very low. This fact coupled with the heat generation rate during a CDA probably means they have a sufficiently fast solubility rate. Of the rare earth oxides, gadolinium oxide (Gd_2O_3) or europium oxide (Eu_2O_3) appears most appropriate. Europium would have a factor of 5 to 10 advantage in neutron cross section. Therefore, europium oxide was the material selected for neutronics investigation to determine the amount of material required to maintain subcriticality of a slumped core.

A series of two-dimensional diffusion theory calculations were performed to determine the amount of europia which would be required to maintain a completely molten core subcritical. Figure 4-1 is a diagram of the basic core configuration. All cladding, duct walls, fuel, and control rods are presumed to have melted. It is postulated that all control and shutdown rods have decomposed and all B-10 has left the core. A molten fuel layer rests on top of a steel-plugged lower axial blanket. Channels have been plugged by solidified cladding. Molten duct wall steel forms the steel pool which overlays the molten fuel layer. Figure 4-2(a) indicates that in excess of 20% by volume of the molten fuel pool must be europia. This equates to over 2 metric tonnes of europia for the demonstration plant. In terms of the essential reaction constituents, the poison-to-fuel mixture equates to about 1.17 kg of europium metal per kilogram of fissile plutonium metal.

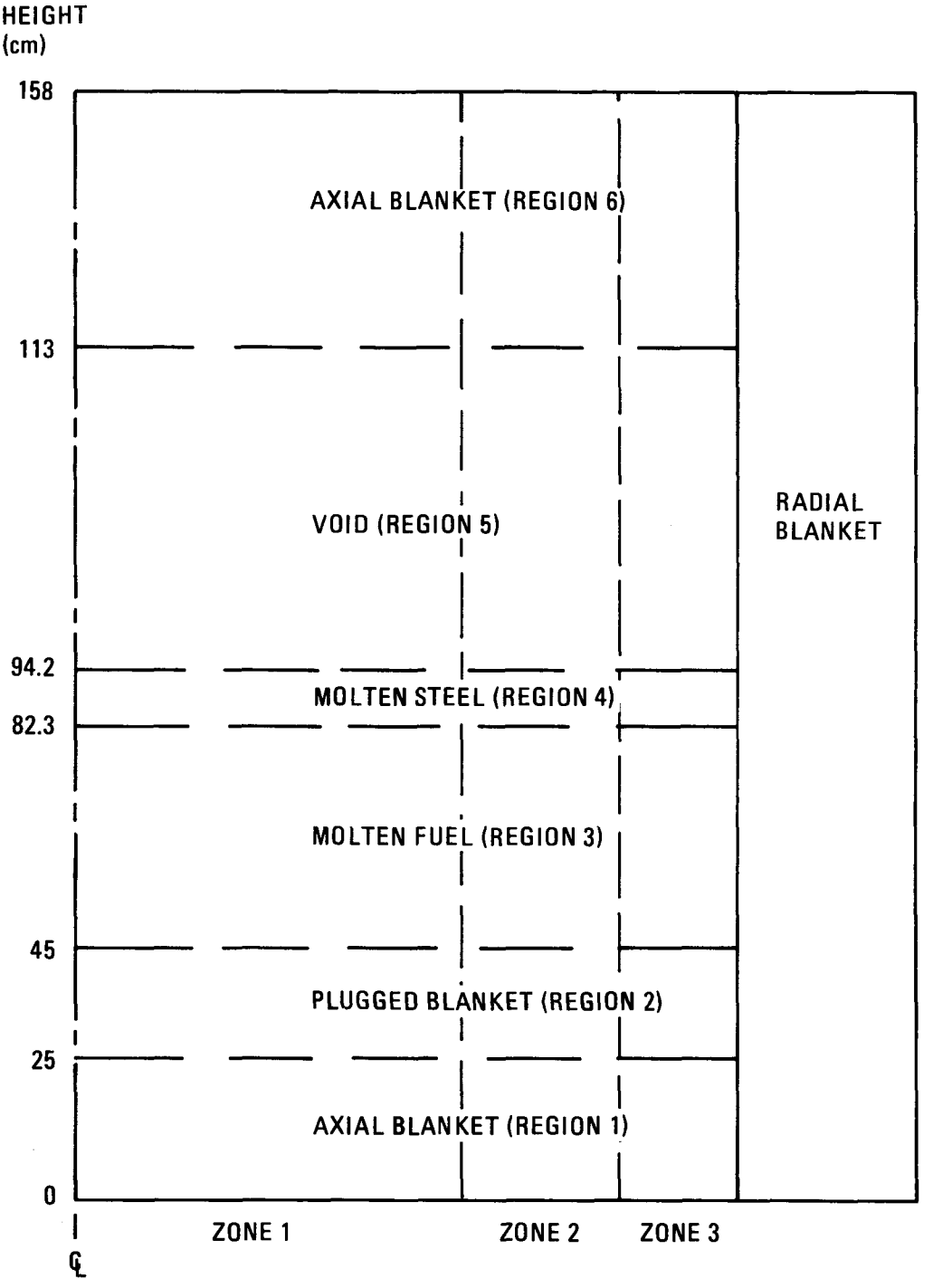

Fig. 4-1. Completely slumped core axial configuration and region heights

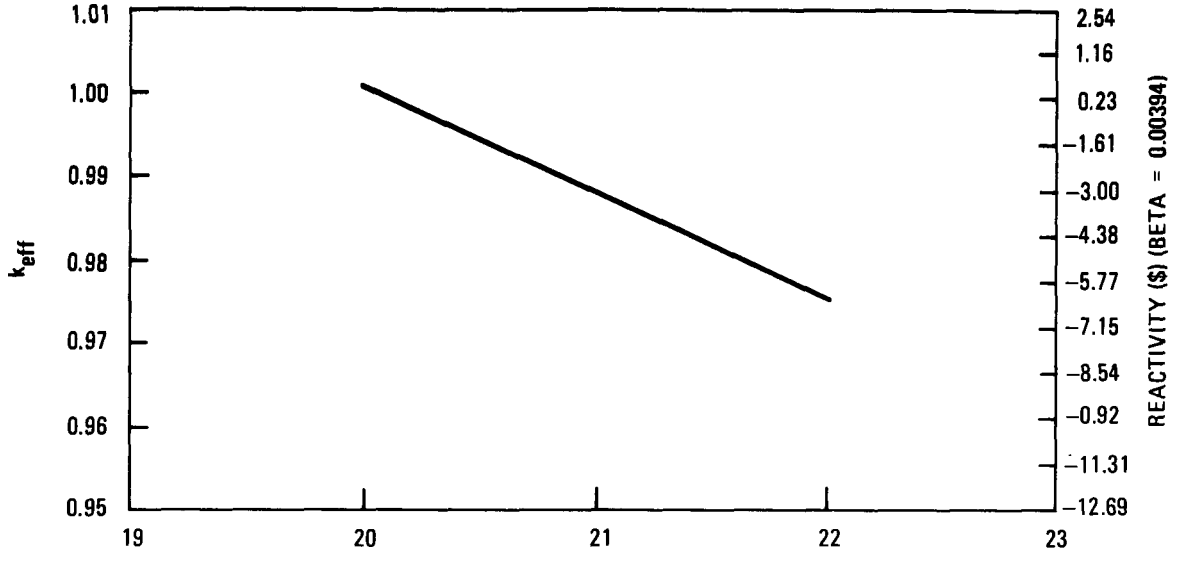

(a) EFFECT OF Eu_2O_3 ON MOLTEN CORE RECRITICALITY

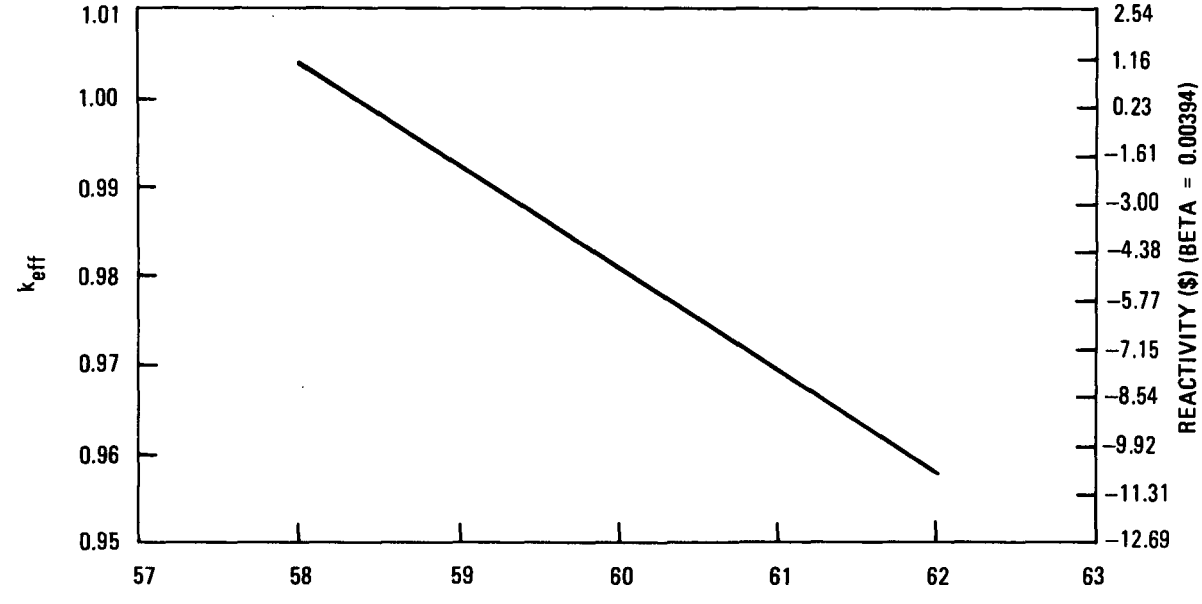

(b) FUEL DRAINAGE REQUIRED TO AVOID RECRITICALITY

Fig. 4-2. Results of poison and drainage criticality studies

While the details of a core poisoning concept have not yet been developed, certain general characteristics would be common. During normal operation, poison pellets or powder would be stored in tubes or baskets partially within the upper axial blanket. Two metric tonnes of europia could be stored in a 60-mm tube with a 1.2-m length in each fuel assembly. The poison would be prevented from entering the core by a linkage arrangement devised to admit it only during a core meltdown.

Accommodation of a 60-mm tube would require the removal of 37 fuel rods in each fuel assembly. If the total fuel inventory is conserved, the breeding and inventory effect of removing the central 37 fuel rods per assembly is minor. The breeding ratio is reduced by less than 5%, the fissile inventory is increased by less than 5%, and the doubling time is increased by less than 30%. If only 19 rods are to be removed by virtue of some future improved concept, the breeding and inventory penalties would appear to be negligible. The effect of placing poison material in the tubes was not assessed.

Much more work would be necessary to determine if a recriticality prevention core poison concept could be mechanically and thermohydraulically achieved without further performance penalties. Furthermore, much analysis and experimentation would be required to establish the viability of a fusable link actuator during an LOSC accident.

4.1.2. Molten Steel and Fuel Drainage

Preventing recriticality during an LOSC by timely drainage of molten fuel is a very uncertain prospect. Two conceptual approaches were investigated. The first postulated that molten steel followed by molten fuel would be able to drain through a tube, similar to the poison tube, in each assembly. This "internal drainage" concept is schematically depicted in Fig. 4-3. The second postulated that molten fuel could spill from a fuel assembly into a control assembly, then drain out the bottom of the control assembly. This "external drainage" concept is schematically depicted in

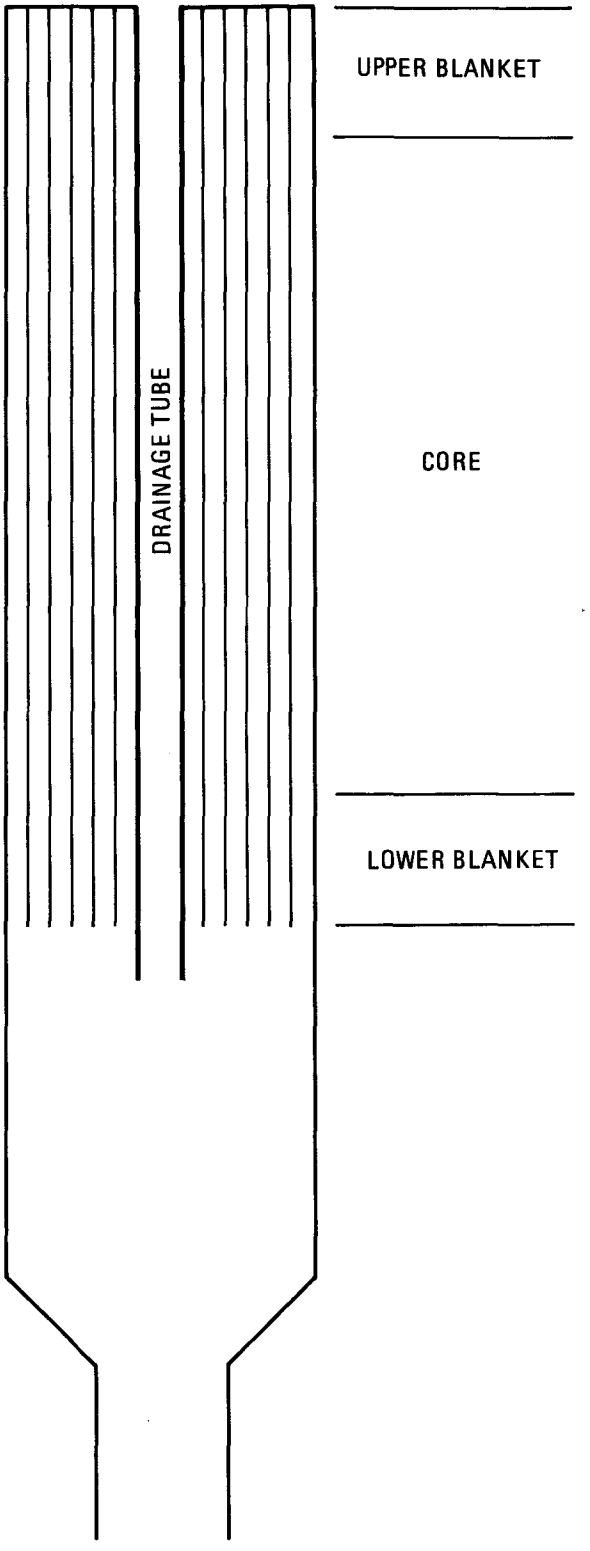

Fig. 4-3. Internal drainage concept

Fig. 4-4. In the current GCFR demonstration plant design, each fuel assembly shares one face of the hexagon with a control or shutdown assembly. The control rod and surrounding fuel rods were assumed to end 50 mm short of the core bottom.

The feasibility assessment addresses three questions:

1. How much fuel must drain completely out of the core and lower axial blanket to prevent recriticality?

2. Can molten steel and molten fuel drain through the available flow paths prior to plugging?

3. Can drainage occur quickly enough to prevent recriticality?

The answers to these questions are summarized in Table 4-1.

The same two-dimensional diffusion theory methodology and configuration (Fig. 4-1) as in the poison study were used to answer the first question. The molten fuel pool height was uniformly lowered over the entire core radius, and successive criticality evaluations were made. The result is shown in Fig. 4-2(b). The initial fully slumped and spread core has a k_{eff} greater than 1.3. About 60% of the core fuel must be removed to assure permanent subcriticality. Another perspective is that a 150-mm-thick molten fuel pool between a layer of molten duct wall steel above and solidified cladding in the lower axial blanket below is critical.

4.1.3. Internal Drainage

The sequence of events leading to internal steel drainage during an LOSC is as follows:

1. Cladding melts, flows down the fuel rods, and solidifies in the lower axial blanket.

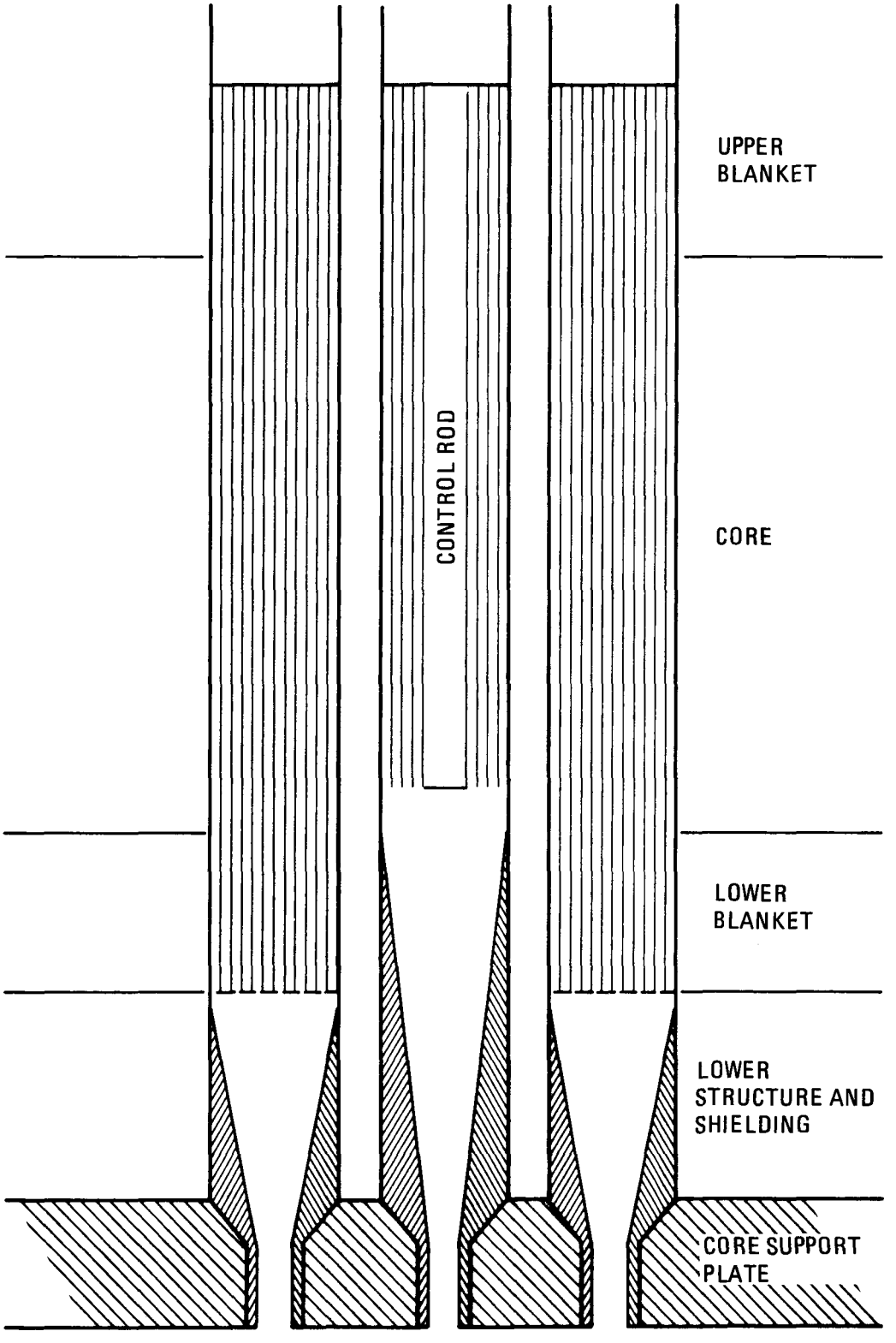

Fig. 4-4. External drainage concept

TABLE 4-1
CONCEPTUAL FEASIBILITY OF DRAINAGE CONCEPTS

	Drains?	In Time?	Feasible?
Upflow external			
Primary concept	No	No[a]	No
Alternate	Yes	No[a]	No
Downflow external	Yes	Yes[b]	Yes
Upflow/downflow			
Internal drains	Yes[c]	Yes	Yes

[a]Recriticality due to fuel slumping may occur prior to draining 60% of the core fuel.

[b]Provided that fuel-crumbling-induced recriticality does not occur.

[c]Tube size is considered too large for a reasonable design.

2. The tube wall begins to melt at the axial midplane.

3. The duct walls begin to melt at the midflat.

4. All coolant channels in the lower axial blanket become plugged with steel, so no further drainage can occur through them.

5. The duct wall melt front progresses axially upward and downward and circumferentially around the assembly.

6. A pool of molten duct wall steel builds up on the steel blockage in the lower blanket at the same time that the tube melt front progresses upward and downward.

7. Molten steel begins to drain into the tube when it has melted down to the molten steel pool level, as shown in Fig. 4-5.

8. After the initial spillover of steel, the rate of steel flow into the drainage tube is governed by the duct wall melting rate because all cladding has already melted and relocated. This provides a maximum mass flow rate of 0.2 kg/s.

This sequence of events was quantified using the SCORIA code, which determined the cladding, tube, duct wall, and fuel temperature histories during an LOSC. Drainage tube sizes ranged from 50 mm i.d. to 135 mm i.d. The former corresponds to removing the central 19 rods from each assembly, and the latter corresponds to removing the central 127 rods from each assembly. Using the above mass flow rate and the SCORIA results, the cladding refreezing model described in Section 3 obtained the results given in Table 4-2. The results assume no flowing helium during steel relocation. Very little steel drains through the lower axial blanket. The tube diameter must be large enough to accommodate solidification of nearly all the duct wall steel and still provide a sufficiently wide path for fuel drainage. If the steel can enter the tube at or above 1477°C with a mass flow rate of at least 0.2 kg/s, then the 135-mm-i.d. tube is

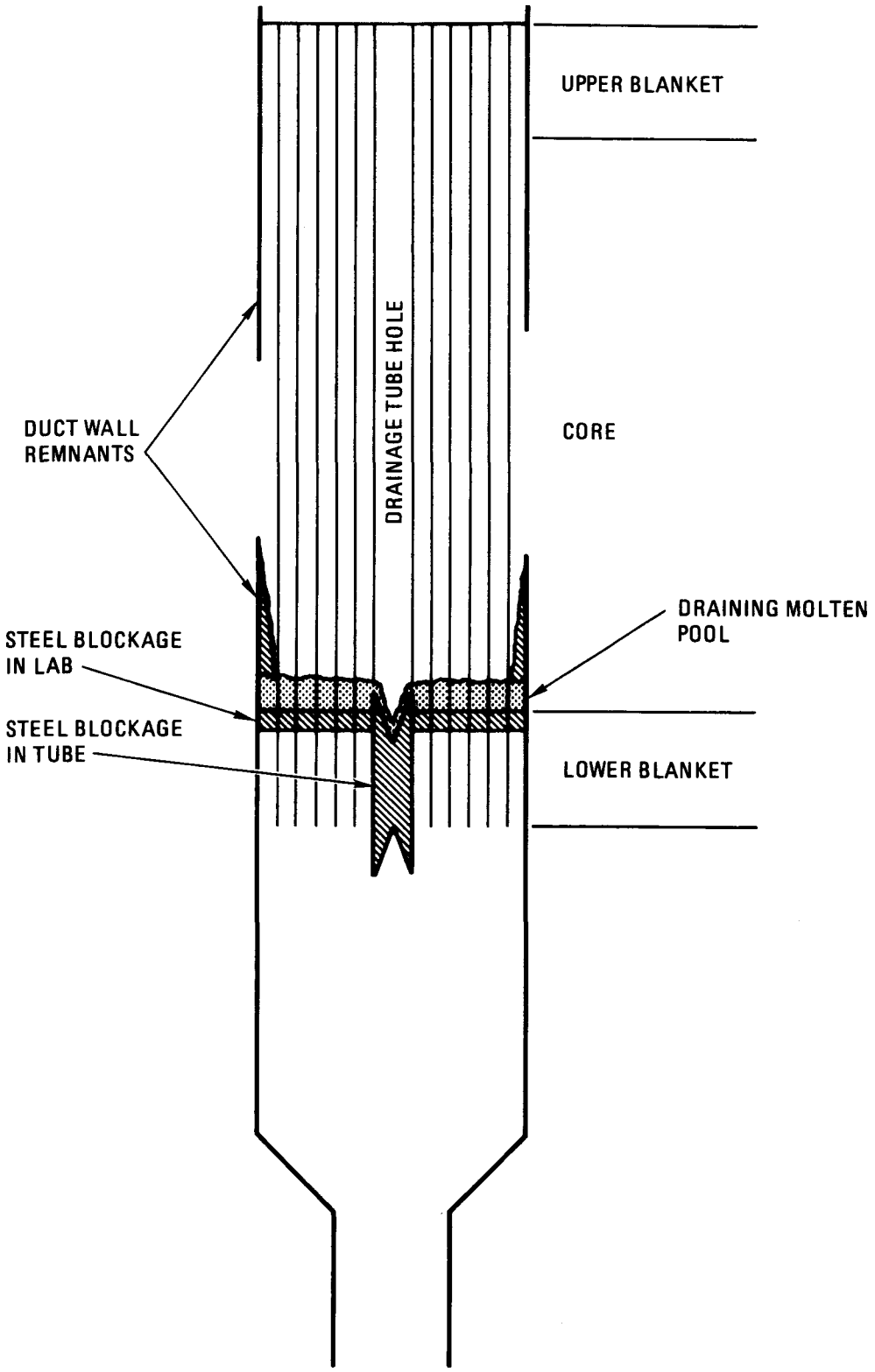

Fig. 4-5. Internal drainage analysis

TABLE 4-2
INTERNAL DRAINAGE ANALYSIS RESULTS
(Same for Upflow and Downflow Cores)

Tube Diameter (mm)	Number of Removed Rods	Minimum Plugging Distance Below Core[a] (mm)
49	19	100^{S}
71	37	100^{S}
92	61	200^{S}
113	91	200^{F}
135	127	Fuel drains

[a] S = plugs with steel only.
F = plugs with fuel and steel; 25-mm gap remains after steel has drained.

sufficient for fuel drainage. If the steel enters the tube with no heat above the liquidus, then more than 127 rods would have to be removed.

4.1.4. External Drainage

The SCORIA code predicts the sequence of events leading to steel and fuel drainage through a control assembly as follows:

1. Cladding melts and flows down the fuel rod toward the lower axial blanket.

2. The cladding blocks the lower axial blanket coolant channels in the fuel assembly but is assumed to drain out of the control assembly.

3. Duct wall melting begins in the fuel assembly, and the melt front spreads axially and circumferentially.

4. Duct wall melting begins in the control assembly.

5. Melted duct wall steel runs down the side of the remaining duct wall and solidifies on the inside duct wall between the core/blanket interface and 200 mm above it.

6. A solidified steel layer as much as 20 mm thick forms on the inside of the duct wall. This substantially slows the downward melting of the duct wall starting 200 mm above the core bottom.

7. The duct wall steel which does not solidify forms a molten steel pool on top of the lower axial blanket blockage.

8. Fuel begins to melt in the fuel assembly.

9. Fuel slumping causes a fuel pool to displace the steel pool overlaying the blockage.

10. The steel pool floats on top of a molten fuel pool.

11. The molten fuel pool increases in height owing to continued fuel slumping.

12. Steel spillover from the fuel assembly to the control assembly occurs when the molten fuel pool elevates the molten steel pool to the elevation of the hole in the duct wall. Spillover occurs between 200 and 350 mm above the lower axial blanket at a rate of about 0.3 kg/s. About 28 kg of molten steel is available for spillover in each fuel assembly.

13. Molten fuel will begin to spill over after all the molten steel has spilled into the control assembly.

14. The available molten steel inventory and 60% of the molten fuel from each cluster of seven assemblies must drain through the control assembly prior to the buildup of a core-wide critical mass.

The STEFINS model described in Section 3 was extended to fuel-on-steel phase change heat transfer. It was used to determine whether the steel followed by fuel could drain through the lower axial blanket region, lower shielding region, and inlet nozzle region of a control assembly. (This would answer the question of drainability.)

Two upflow inlet nozzle and shielding configurations were investigated. The lower axial blanket region which had all rods removed by design (Fig. 4-4) was the same for both the upflow and downflow cases. The downflow core did not have any additional shielding. The results show that both steel and fuel could drain out of the downflow control assembly without plugging. Figure 4-6 shows the results superimposed on the mechanical latch design of the upflow inlet nozzle. Steel almost plugs the space at the elevation where the assembly passes through the core support plate. This starts about 650 mm below the core/lower blanket interface.

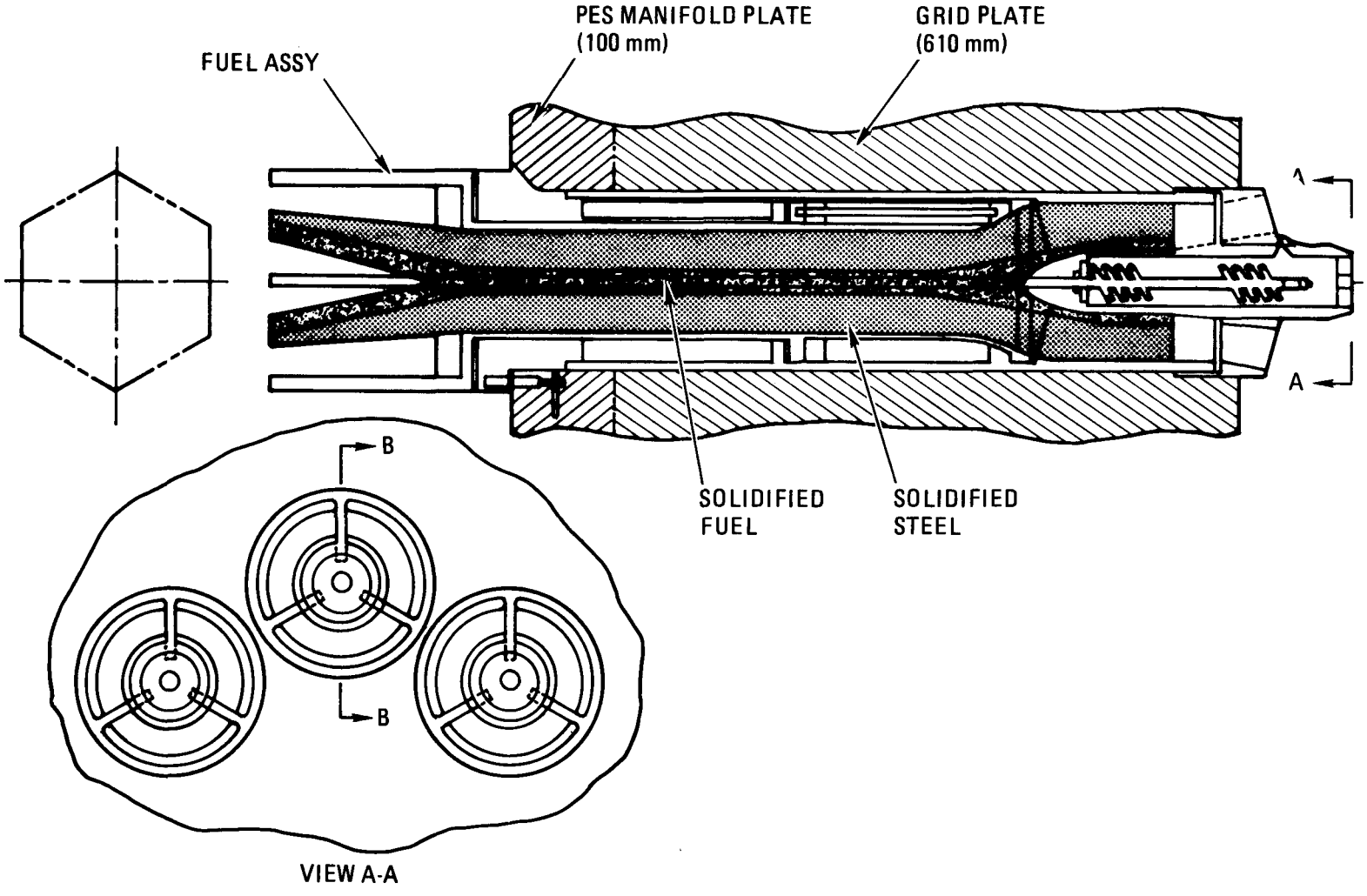

Fig. 4-6. External drainage analysis of primary design

The remaining 11-mm hole is quickly plugged by the buildup of a solid fuel crust as molten fuel tries to flow through the hole.

Only a small amount of steel actually flows out of the assembly. It freezes and builds up a layer within the nozzle and shielding region. A more suitable inlet nozzle configuration for drainage would be one which can accommodate the solidified steel while maintaining a residual flow path large enough for fuel to drain. The hole must be large enough to accommodate some fuel solidification as well. Therefore, an alternate upflow inlet nozzle configuration was investigated. This configuration removed the mechanical latch and widened the coolant passage. Figure 4-7 shows the analytical results superimposed on the alternate design. This design has the potential for allowing drainage without plugging.

The crucial consideration is whether 60% of the fuel can be removed before recriticality (question 3). Table 4-3 demonstrates the drainage timing. Spillover occurs when the molten fuel layer elevates the molten steel layer to the opening in the duct wall. Therefore, the molten fuel layer must be between 150 and 200 mm thick. This range encompasses the amount of fuel slumping, over the whole core, required to cause recriticality. Therefore, on the average the core is likely to reach its recriticality configuration before reaching its spillover configuration. Although the hot assembly begins to drain prior to predicted recriticality, the coldest 50% of the fuel may not sufficiently drain until after recriticality. Hence, external drainage is not likely to prevent recriticality and is not by itself considered a feasible accident mitigation concept for either the upflow or downflow design. Delay of criticality by timely addition of more neutron absorber material may allow sufficient time for fuel drainage.

4.1.5. Fallaway (Downflow Core Only)

Individual or small group assembly fallaway is an accident mitigation mechanism, unique to the downflow core, which can prevent criticality. It

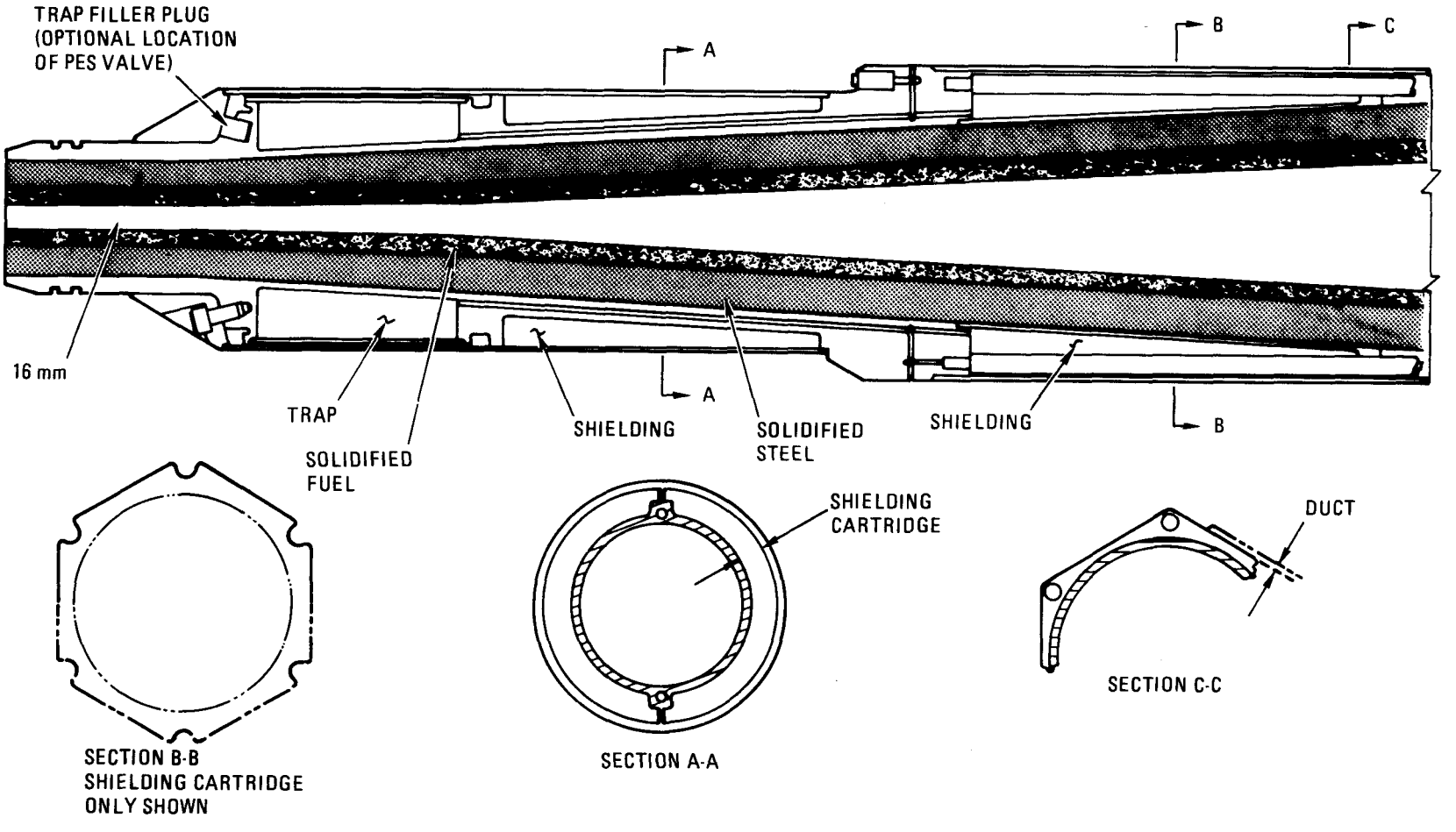

Fig. 4-7. External dainage analysis of alternate design

TABLE 4-3
EXTERNAL DRAINAGE TIMING[a]

	Hot Assembly (s)	Coldest 50% of core (s)
Steel spillover into interduct spacing	570	690
Fuel melting	650	770
Steel spillover into control assembly	670	790
Fuel spillover into control assembly	720	840
Sufficient fuel drainage[b]	900	1020
Slumped core criticality	970	970

[a]Drainage requires 60% of the core fuel to be removed for permanent shutdown.

[b]Using average calculated fuel spillover rate of 0.3 kg/s.

currently appears that only a very small performance penalty accompanies the somewhat increased interduct spacing necessary for fallaway feasibility. Feasibility could have been demonstrated in the DMFT program at LASL.

The sequence of events leading to fallaway during an LOSC is as follows:

1. Cladding melts, flows down the fuel rods, solidifies near or in the lower axial blanket, and blocks the coolant channels.

2. Welding of one rod to another and fuel rods to the tie rods may occur.

3. The dead weight load from declad fuel columns, the relocated cladding, the lower axial blanket, and duct walls is transmitted through the blockage, through the tie rods, and up to the fuel rod support grid above the upper axial blanket.

4. Therefore, the tie rods are loaded in tension and would be expected to fail at their hottest, weakest elevation.

5. The duct walls begin to melt at the midflat a few seconds before corner tie rods fail.

6. Upon tie rod failure, the dead weight load of the assembly may be temporarily transmitted through the duct wall to the core support plate. Since the duct wall has already started to melt, it would be expected to fail shortly after the tie rods.

7. At this time, the assembly wall below the core midplane would drop from the core, followed by the unsupported fuel columns, lower axial blanket, and relocated steel.

The corner tie rods are expected to fail when they reach approximately 1100°C. At this time very little duct wall melting will have occurred. Therefore, molten steel spillover into the interduct spacing is not expected. Relocating tie rods to the midflat line would increase the time delay between fallaway and any potential spillover.

Since spillover may be eliminated as a potential fallaway inhibitor, it is relevant to determine if direct duct-to-duct interference would prevent fallaway. Fuel assemblies provided with an interduct spacing greater than 13.3 mm cannot be restrained from falling by bridging loads between the assemblies. The falling fuel assembly is not expected to be stopped by its own distorted shape or distortions of adjacent fuel assemblies. The following paragraphs describe the fallaway interference analysis.*

Duct walls which have begun to melt will fall, upon tie rod failure, unless restrained by adjacent ducts. Bridging is one means of restraint and is caused by dilation, swelling, and thermal expansion. Another possible mechanical restraint is from adjacent duct bowing owing to thermal gradients and relaxation of cold work. Adjacent ducts generate a normal force on the falling duct that is limited by their geometry and temperature. The worst case creep, swelling, and thermal expansion conditions from a NUBOW code (Ref. 4-1) steady-state irradiation analysis of the GCFR core was used for the bridging investigation. An interduct gap width greater than 13.3 mm would prevent bridging.

The restraining force generated by deformed adjacent ducts was compared with the restraining force required to stop a falling duct. The product of the restraining force and the coefficient of friction must exceed the dead weight of that portion of the falling assembly which is supported by the lower axial blanket blockage. Since azimuthal temperature symmetry was assumed, the restraining force can be developed only if there are two ducts on opposite sides of the falling duct. In effect, a

---

*The authors wish to acknowledge A. Lewis of General Atomic Company for the fallaway interference analysis.

"pinch" force is exerted on the falling duct. It was found that the maximum restraining force normal to the falling duct is 1197 N located at the assembly bottom. A friction factor of 1.1 will provide sufficient upward force to prevent fallaway. This is somewhat greater than expected friction factors if adjacent ducts have not touched during normal operation, but less than possible if long contact periods have occurred. However, the force has a maximum value which is a function of the fully developed plastic hinge at the hottest elevation of the adjacent ducts. The plastic hinge is defined as a section in bending where half of the material is at the tensile yield stress and the other half is at the compressive yield stress. Therefore, the pinch force cannot be maintained over a significant length of time because of creep relaxation of the adjacent ducts which have temperatures above 1200°C.

The breeding performance impact of a 15-mm interduct spacing has been found to be comparable to that of removing the central 19 rods in each assembly, as discussed with respect to poison mitigation. The uncertainties that should be resolved or verified before duct fallaway can be considered a viable concept are:

1. The possibility that fuel crumbling may lead to recriticality before duct fallaway. Data on fuel pellet bonding from out-of-pile tests are needed. Fuel crumbling may be integrally tested in a 7- to 37-rod bundle.

2. The confirmation of the interduct gap required to assure no mechanical binding.

3. Demonstration that no steel spillover occurs before duct melting on the control rod side. Current analysis indicates no spillover.

4. Investigation of the influence of upward heat transport by intra-assembly and interassembly natural convection.

4.2. PAFC COMPARISONS

Based on analyses and current design configurations, the PAFC functions of the upflow and downflow designs were evaluated. These evaluations led to the final PAFC recommendations for the GCFR demonstration plant.

4.2.1. Conclusions from In-Vessel and Ex-Vessel PAFC Analyses

The upflow core analysis precluded heat removal from the core support plate and radial shield by helium convection. The downflow analysis permitted convection heat removal. Hence, the upflow core support plate was calculated to fail, while the downflow radial shields and core support plate were not. Therefore, the availability of convection heat removal from the PCRV internal structure to the helium was shown to be an important factor in determining the MFCS requirements on the PCRV floor.

Based on the assumptions, more heat removal mechanisms are available to the downflow design, with only cavity liner cooling being permitted for the upflow design. However, based on the heat transfer results for the upflow design without helium convection, the upward heat removal through the cavity liner, though marginal, looks encouraging. The parametric studies further show that the thermal margin can be extended by several design modifications.

Ex-vessel analyses identify tendon failure as the earliest threat to PCRV integrity for both the upflow and downflow designs if neither an MFCS nor cavity liner cooling is provided. Fuel spillover into the side cavities in the upflow design adds another failure mode to the PCRV. However, spillover is not significant in the absence of cooling because melt-through of the lower cavity liner occurs much earlier than spillover. With sufficient liner cooling, spillover becomes the only failure mode of the PCRV for the upflow concept. Therefore, prevention of core support plate and radial shield structural failure in an upflow design is quite

important. Molten fuel ingress into the refueling penetration gaps remains a failure mode for the downflow concept.

4.2.2. Evaluation of In-Vessel Versus Ex-Vessel PAFC

The technical bases for evaluating in-vessel versus ex-vessel PAFC for both the upflow and downflow designs are as follows:

1. Exposure of PCRV tendons to molten fuel. Before penetrating deeply into the PCRV base slab, molten fuel would attack the PCRV tendons and cause them to fail. To prevent ejection of the central cavity closure, the PCRV would need to be depressurized at the time of tendon overheating.

2. Retention volume for debris. An in-vessel MFCS has to contain the debris from melted core, shielding, and structural material inside the central cavity only. An ex-vessel MFCS must, in addition, contain the molten concrete from the PCRV base slab which forms a solution with the molten fuel. The retention volume for an ex-vessel MFCS is 5 to 10 times larger than for an in-vessel MFCS.

3. Liner failure and water ingress. The increased temperature of the liner and liner cooling tubes just prior to liner failure is expected to cause boiling in the tubes. This would tend to minimize the amount of water ingress.

4. Bottom penetrations. Analyses presented in this report indicate that molten fuel entry into the gap between the penetration and the base slab will not lead to early failure and ejection of the plug.

5. Hydrogen generation. Water released from concrete after liner failure in the absence of all liner cooling is expected to rise

as vapor up through the debris pool and react with the overlaying steel layer to form hydrogen. It is expected that a recombiner will be required to prevent the accumulation of an explosive mixture.

6. Bottom head failure. The eventual failure of the PCRV bottom head is an inherent feature of an ex-vessel MFCS. At the time of failure it must be assured that the PCRV is pressure equalized with the containment, or alternatively the MFCS must be designed for the pressurized ejection of core debris to prevent the distribution of this debris throughout the containment by blowdown forces.

The technical aspects of this evaluation are summarized in Table 4-4. An ex-vessel MFCS would require major design changes in several areas, and their feasibility must be assessed before any ex-vessel molten fuel containment approach can be declared fully feasible.

Thus, the recommendation for an in-vessel MFCS is principally based on:

1. Avoiding all the difficulties associated with an ex-vessel MFCS approach.

2. Avoiding the introduction of a new cooling system. An in-vessel MFCS would use (in a modified form) the liner cooling system for the lower central cavity, whereas an ex-vessel MFCS would require its own cooling system.

3. Using the PCRV as a massive structure for containment and shielding of the debris, allowing only gaseous and volatile fission products to escape into the containment.

TABLE 4-4
SUMMARY OF IN-VESSEL VERSUS EX-VESSEL MFCS EVALUATION

Phenomena	MFCS Location			
	In-Vessel		Ex-Vessel	
	Downflow Core	Upflow Core	Downflow Core	Upflow Core
Tendon attack	No concern	No concern	Potentially unacceptable consequences Significant design changes required	
Retention volume	Small	Medium	Large	
Liner failure and water ingress	No problem	No problem	No major difficulty expected	
Bottom penetrations	Design solution simple and practical	No problem	Penetration failure delay of 30 hr	
Hydrogen generation	No problem	No problem	Requires recombiner to protect containment	
Concrete decomposition	No problem	No problem	Requires no-limestone aggregate in PCRV bottom head	
Bottom head failure	No problem	No problem	Requires prior PCRV-containment pressure equalization	
MFCS design feasibility				
Material selection	Limited	Limited	More material flexibility	
Heat fluxes	Large	Medium-large	Smaller	
Technical feasibility	No serious feasibility concerns have been identified to date for any option.			
Technical difficulty	Substantial	Substantial	Probably less difficult	

4.2.3. Evaluation of Molten Fuel Containment Concepts

Post-accident fuel containment concepts for the GCFRs have been developed in Germany (Ref. 4-2) and in the U.S. (Ref. 4-3). Among the many concepts, the ceramic crucible, the borax bath, the uranium metal bath, and the steel bath concepts have been studied for the GCFR. The analytical methods used for the evaluation of alternate concepts include Baker's empirical model (Ref. 4-4) for two-dimensional heat transfer in internally heated pools, conduction heat transfer through the side and bottom structures, and convective and radiative heat transfer from the pool surface to the PCRV internal structures.

The ceramic crucible utilizes a buildup of refractory material, forming a crucible inside the liner to contain the molten core debris without melting or chemical attack of the crucible surface and at the same time providing the required shielding for normal operation. Previous analyses (Ref. 4-3) for a 300-MW(e) GCFR have shown that this concept can be applied to the current GCFR design with minor modifications. The thick crucible wall provides a stored heat capacity that can last some 30 hr after core meltdown. The peak heat flux which eventually reaches the cavity liner is sufficiently low so that only a moderately enhanced liner cooling capacity will remove the entire downward flowing heat. However, because of the thick crucible wall, the debris pool temperature reaches 3000°C and the margin for fuel boiling under depressurized conditions is small. Also, most of the core debris decay heat is driven upward, which makes this concept highly dependent on upward heat removal. In addition, design provisions would be required to avoid the flotation of crucible blocks in the fuel pool.

The borax bath concept was proposed by Dalle Donne et al. (Ref. 4-5) for the GCFR. Steel boxes filled with borax ($Na_2B_4O_7$) are installed in the lower reactor cavity. Following a core meltdown, the oxide fuel is expected to dissolve in the liquid borax to form a compound solution pool. The dissolving process is controlled by steel box melting, so the liquid

borax is already at the melting point of steel where a fast dissolving rate may be achieved. The low boiling point of borax (1700°C) may cause a borax vapor blanket to form at the fuel/borax interface, so the fuel and steel may sink through the borax bed without dissolving the fuel. In addition, the borax pool may become separated from the fuel by an intermediate steel layer to interrupt the dissolving process. Small-scale simulation tests performed by Dalle Donne et al. (Ref. 4-5) indicate that UO_2 dissolution can be accomplished in the presence of steel, and larger experiments are currently in progress. Only 20% to 30% of the decay heat flows upward because of the low pool temperature. Sideward and downward heat fluxes are increased, but the peak heat flux does not occur for about 10 hr.

The heavy metal bath concept utilizes a large mass of high-density, low-melting-point uranium metal alloy installed inside the lower reactor cavity. Following a core meltdown, a low-temperature pool of the uranium alloy is expected to form with solid fuel fragments in suspension. The molten pool will be contained by the unmelted solid edge of the heavy metal. The principal advantage of this concept is its self-sealing feature. Air gaps between structural alloy blocks will become filled by the uranium alloy, which is of higher density than UO_2, thereby preventing the penetration of molten UO_2 into structural gaps and cracks, which otherwise can locally increase the heat flux to the cavity liner. A heat transfer study (Ref. 4-6) for the 1540-MW(e) GCFR has shown that heat removal from the heavy metal bath is feasible with a wide range of suitable pool temperatures. Disadvantages of this concept include the high cost of uranium materials, the potential for metal-water reactions if the liner is breached, and the possibility of crusting on top of the heavy metal that could suspend a significant fraction of the UO_2 above the pool. Uranium alloys also have a low heat capacity requiring a 2-mm-thick layer for a 4-hr heat capacity.

A steel bath concept employs a large mass of stainless steel plates that will melt following a core meltdown to form a "light metal bath."

This concept is similar to the uranium metal bath except that the core debris is heavier than the pool material and will be collected at the bottom of the steel pool. A refractory layer placed between the steel and the cavity liner is thus needed to protect the liner from potential hot spot effects. Analysis of the steel bath heat transfer (Ref. 4-7) has shown that a steel core retention system has a greater stored heat effect than the uranium system and therefore the liner heat flux and temperatures are lower. Similar to the ceramic crucible concept, this concept can be accommodated without a large cost or significant design changes.

The four molten fuel containment concepts discussed above may be classified as either a crucible type or a pool type containment system. The ceramic crucible is a crucible type system, while the remaining three are pool type systems. Crucible type systems apply a permanent crucible material to contain the molten fuel without melting or chemical attack of the crucible surface. Pool type systems apply a large quantity of sacrificial materials to form a molten pool so that the decay heat sources are diluted. The large cooling surfaces provide a greater sideward heat removal so that the upward heat removal is reduced.

The crucible concept would be a natural choice for an existing GCFR design because of its low cost and simplicity. Only minor design changes would be required, whereas for the pool concepts, major design changes would be anticipated. Also, the heat transfer mechanism in the molten pool for a ceramic crucible, containing only fuel and steel, has been extensively experimentally investigated. Experimentally verified heat transfer correlations are available for practical use. The feasibility of the pool type concepts has less experimental demonstration. Scaleability is also better for the crucible concept than the pool concepts because of the relatively straightforward potential enhancement of liner cooling capacity. However, a mechanism to remove the large fraction of upward directed decay heat must be provided for the crucible concept, whereas only a small fraction of the total decay heat is directed upward in the pool concept. Upward heat removal for the pool concept may be accomplished by the cavity liner cooling system in the upper cavity.

The heavy metal bath system inherently eliminates the possibility of fuel penetration and material flotation. These problems remain for the borax bath and steel bath systems. The melting process in forming a metal bath (heavy metal bath and steel bath) appears more dependable than the dissolving process in forming a compound solution pool (borax bath). Both the heavy metal bath and the steel bath concepts can be managed in a wider pool temperature range than the borax bath concept. In the borax bath concept, the pool temperature is limited to a narrow range by both the dissolution rate of oxide fuel in borax and the evaporation rate of borax. The main disadvantage of the heavy metal bath concept is the limited availability of suitable materials. Uranium metal and its alloys are excellent in most properties except heat capacity but have a penalty of high cost. Borax and steel are readily available at low cost.

The steel bath concept has a larger specific heat capacity and lower material cost than the uranium bath concept and a wider pool temperature tolerance than the borax bath concept.

Table 4-5 compares the important parameters of the molten core retention concepts. The ceramic crucible is the simplest concept but is highly dependent on upward heat removal, whereas the borax bath and uranium bath concepts offer better performance but would require major design changes and experimental development. The steel bath concept appears to be an interesting compromise. Furthermore, a combination of the essential features of two concepts, i.e., heavy metal base with an overlaying steel bath, may offer further improvements. It is concluded that several diverse concepts for molten fuel containment inside the PCRV are feasible and would exploit the normally provided cooled liner barrier for PAFC.

4.2.4. Upflow Versus Downflow PAFC Evaluation

The upflow and downflow concepts were evaluated using a set of 19 desired PAFC functions. Table 4-6 lists these functions and indicates which are relevant to an upflow versus downflow design comparison. Table 4-7 summarizes the major differences between the upflow and downflow concepts which are significant to a PAFC comparison.

TABLE 4-5
COMPARISON OF MOLTEN CORE RETENTION CONCEPTS

Parameter	Ceramic Crucible Concept	Borax Bath Concept	Uranium Bath Concept	Steel Bath Concept
Pool temperature, °C	High (>3000)	Low (1427)	Low (>1200)	Low (>1500)
Cavity liner temperature, °C	Low (150-200)	High (300-400)	High (280-350)	Medium (250-300)
Time of maximum liner heat flux, hr	Long (20-40)	Medium (6-10)	Short (3-4)	Medium (6-10)
Maximum liner heat flux, kW/m^2	Low (50-100)	High (200-300)	High (200-300)	Medium (150-250)
Fraction of upward heat removal	High (0.6-0.8)	Low (0.2-0.3)	Medium (0.3-0.4)	Low (0.1-0.3)
Design changes needed	Minor	Major	Major	Minor
Need for experimental work	Low	High	High	Medium
Pool manageability	Medium	Low	High	High
Fuel penetration and material flotation	Yes	Yes	No	Yes
Scaleability	High	Low	Medium	Medium
Cost	Low	Medium	High	Low

TABLE 4-6

PROBLEMS INVOLVED IN PAFC DESIDERATA

Desideratum	Upflow	Downflow
1. Containability	X[a]	X
2. Initial conditions	X	X
3. Secondary melting	X	X
4. Containment duration	X	X
5. Retention volume	X	X
6. Debris entrance	X	X
7. Fuel boiling		
8. Material compatibility	X	X
9. Structural compatibility		
10. Criticality control		
11. Cavity liner failure		X
12. Concrete failure		
13. Flotation	X	X
14. PAFC cooling	X	X
15. Availability, operability, reliability	X	X
16. Scaleability	X	
17. Neutron and thermal shielding		X
18. Refueling		X
19. Normal operation service requirements		

[a]X signifies a unique upflow or downflow problem exists.

TABLE 4-7
MAJOR PAFC-RELATED DIFFERENCES BETWEEN UPFLOW AND DOWNFLOW DESIGNS

Design	Difference	Consequence
Reactor Vessel System		
PCRV structure	UF: Upper penetration DF: Lower penetrations	— Weakens lower PCRV
Cavity liners	--	—
Liner cooling	--	--
Thermal barriers	UF: Thicker in upper cavity DF: Thicker in lower cavity	Upward heat removal reduced Downward heat removal reduced
Fuel Handling System		
Penetrations	UF: Above the core DF: Below the core	— Open during refueling Seal presents a weak point
Core position	UF: Low in cavity DF: High in cavity	Natural convection feasible Greater falling distance Single refueling assembly drop
Reactor Internals System		
Core support	UF: Grid plate below the core	More material for base case melt Higher temperatures from transition phase Initial conditions uncertain Greater mass falling on MFCS Grid plate fails faster Greater pool depth Aids lower shielding
Core barrel	DF: Grid plate above core	Failure requires more containment volume Grid plate protected by assemblies Fuel enters MFCS sooner Inhibits intracavity convection Possible fallaway
Shielding	UF: Shield material in assemblies DF: Shielding materials massive	Better shielding Failure requires more containment volume
Reactor Core System		
Fuel assembly	UF: More fuel More steel More shield DF: Less material	More material for minimum containment volume requirement More material for minimum containment volume requirement More material for minimum containment volume requirement Limited upward heat removal Graphite reactions Smaller MFCS
Cooling Systems		
Steam generators	UF: Duct in lower cavity DF: Duct in upper cavity	Spillover —
Safety conditions	UF: Less cooling mechanisms available DF: 1 CACS loop available	Less upward heat transfer Pool design needed Crucible or pool design possible

The PCRV lower head in the downflow concept is less effective than that in the upflow concept because of the refueling penetrations. In fact, during refueling a downflow MFCS would not be available because the refueling plug would be removed. The minimum required MFCS volume of core and blanket material for the downflow concept is somewhat less than that for the upflow concept; but the maximum is somewhat more for the downflow concept because of the more massive radial and lower central cavity shielding. If heat transferred in the upward direction from the molten debris must be removed solely by the cavity liner cooling system, then a pool type concept is preferred. However, this concept requires additional experimental information, while the crucible concept does not. Another consideration is the potential for fuel to spill into the side cavities through the inlet ducts in the upflow concept. However, it may be feasible to raise the elevations of these ducts to eliminate that concern.

In conclusion, no major feasibility problems with PAFC have been identified for the in-vessel crucible or pool type concepts. Both the upflow and downflow PAFC concepts could be made feasible with proper design and experimental heat transfer information.

The most important technical considerations for the downflow concept are the ingress of molten fuel into the refueling penetration and the unavailability of the MFCS during refueling. The most important design consideration for the upflow concept is the potential for spillover of molten core debris into the side cavities.

As a direct consequence of the assumptions, the downflow design provides better heat removal. However, the upflow design has better containment capability. Since design margins exist to improve the heat removal but containment capability is inherent, the upflow design is considered slightly better than the downflow design.

4.3. FLOW BLOCKAGE ACCIDENT

An incident initiated at full power and full flow by a complete flow blockage of an individual subassembly is of interest because of the potential for damage propagation from one subassembly to another. It is expected that the probability of such an occurrence would be made exceedingly low by design for both an upflow and a downflow core. It is also expected that instrumentation would be provided to enable reactor shutdown before damage spread to an adjacent subassembly. Scoping studies at General Atomic indicate that over 90% of the subassembly inlet flow area must be blocked in order to cause cladding melting. Nevertheless, the event sequence diagram (Fig. 4-8) presumes a complete flow blockage at full-power operation. Although a flow blockage analysis has been presented in Chapter 15 of the GCFR Preliminary Safety Information Document (PSID), some portions were reanalyzed to include better modeling for cladding and fuel relocation and for convection heat transfer in a molten pool.

Within the assembly which is blocked, the initial few seconds are similar to an unprotected LOF accident in a low-power subassembly. The damage propagation mechanisms would be blockage of flow channels by cladding and fuel relocation and solidification and thermal attack of the duct wall by molten fuel. If these mechanisms cause subsequent melt-through of the duct wall of unblocked subassemblies, the phenomenological questions would be similar to those of fuel sweepout in a TOP.

Following a complete flow blockage of an individual subassembly, cladding would begin to melt within a few seconds. Fuel would begin to melt soon afterward. If relocated cladding or fuel blockages formed near the core bottom, the duct wall would eventually succumb to thermal attack by contact with molten fuel. The downflow core blocked fuel assembly could then fall from the core, thereby preventing further damage propagation. However, if molten material cannot drain through the interduct spacing (and through the lower support structure), the adjacent duct walls

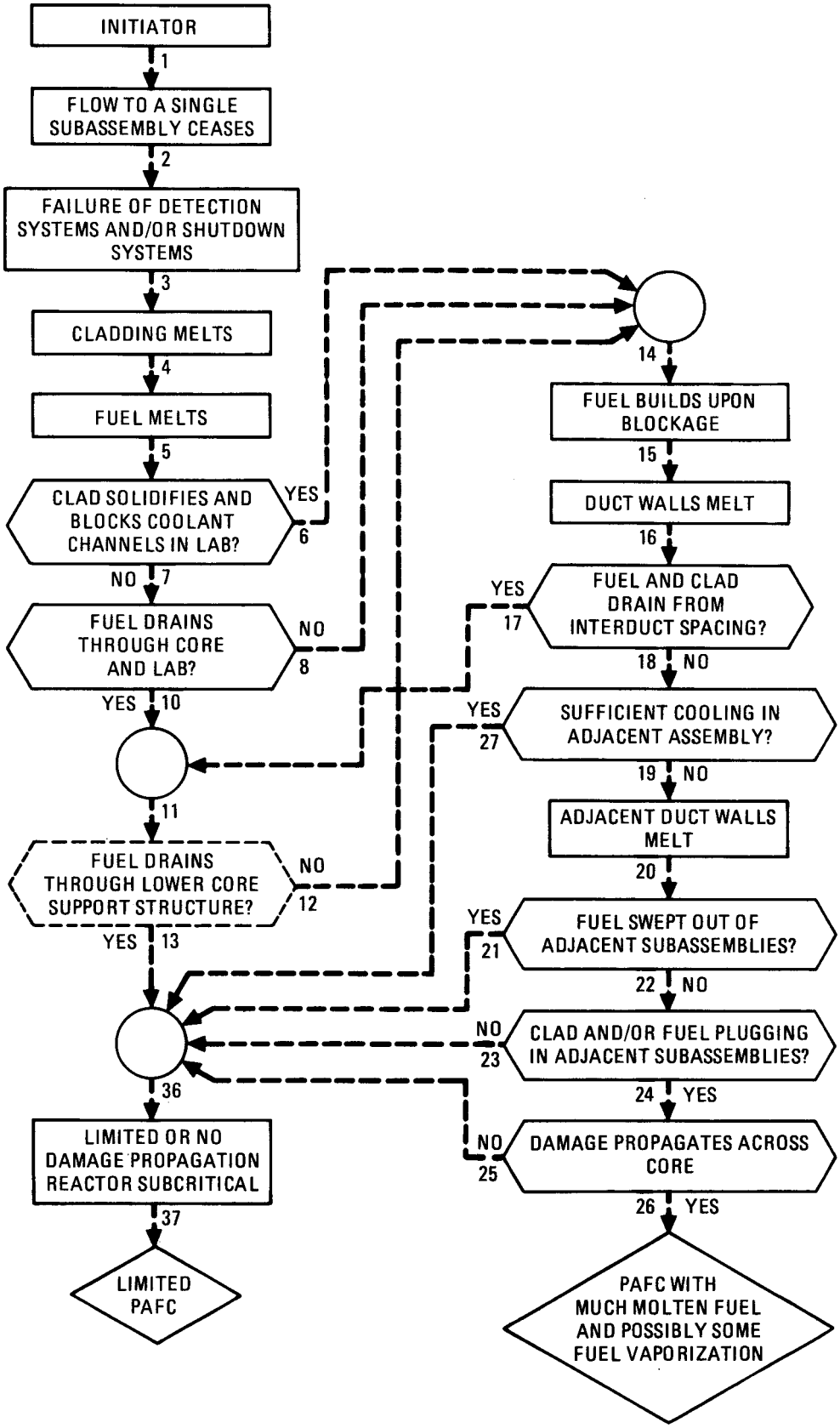

Fig. 4-8. Total flow blockage of an individual subassembly in an upflow core

of surrounding subassemblies may eventually melt. Since these subassemblies have residual flow, molten fuel may or may not be swept out of the subassemblies in both upflow and downflow concepts similar to the situation after cladding failure during a TOP. Similar to a TOP, it is only in the event that fuel sweepout is not effectively attained that damage can spread beyond the adjacent duct walls.

It was found that cladding blockages in the lower axial blanket similar to those during an LOSC may form. A molten fuel pool would build up and begin to melt through the duct wall of the blocked asssembly. Assuming a 10% residual flow after reactor trip, the duct walls in the unblocked, adjacent assemblies are calculated to melt. This sequence would lead to welding together of the seven-assembly group which has the blocked assembly at its center. The sequence of events beyond duct melting is highly uncertain. The relatively short time between detection and damage propagation appears to preclude operator intervention.

Table 4-8 compares the event sequence and timing for the upflow and downflow cores assuming no early accident termination mechanism. A downflow core designed for fallaway during an LOSC would automatically provide an early accident termination mechanism without damage propagation. The buildup of a molten fuel pool prior to duct wall melting is a condition more favorable to the success of fallaway than the LOSC conditions. When the molten pool had raised the duct wall and tie rod temperatures to their yielding points under the assembly weight, the assembly would drop from the core. This would occur before melting of neighboring assemblies. An early accident termination mechanism for the upflow core has not yet been identified.

The computer programs SCORIA and STEFINS predicted the following sequence of events in the blocked assembly using the PSID power transients as shown in Fig. 4-9:

1. Flow completely and instantly stops in a single assembly at t = 0.

TABLE 4-8
FLOW BLOCKAGE ANALYSIS SUMMARY

	Time (s)	
	Upflow	Downflow
Initial clad slumping	2	2
Initial fuel slumping	6	6
Onset of molten fuel pool thermal attack on duct wall	9	8
Scram time	10	10
Time to melt first wall adiabatically	13.8	12.7
Time to melt first duct wall with flow[a] in adjacent assembly	16	15
Time to melt through duct wall in adjacent assembly (propagate damage) with flow	22	21
Conclusion: Damage propagation will occur unless the assemblies fall away upon duct wall melting.		

[a]Average flow rate during the duct wall melting sequence is 10% of full flow.

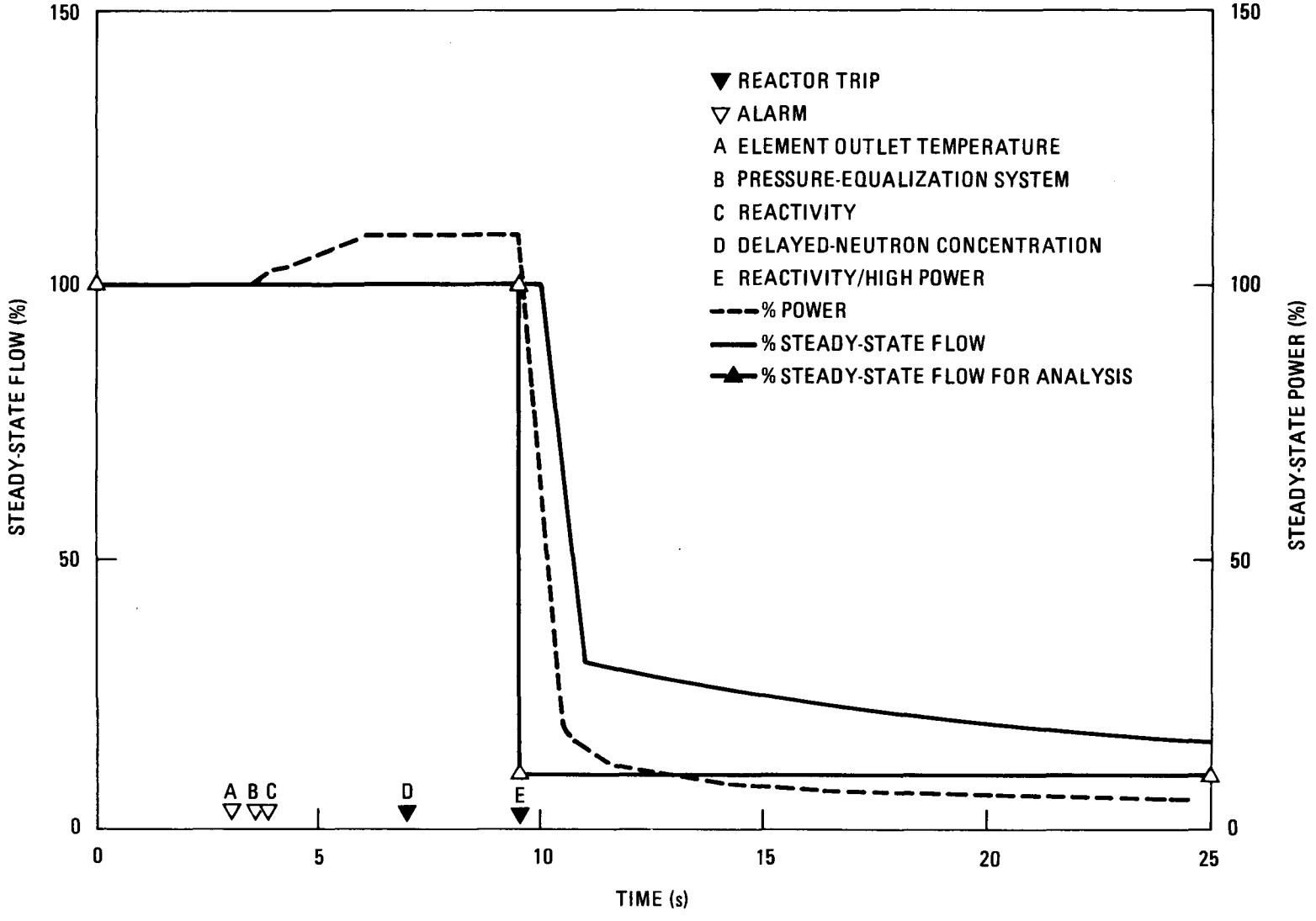

Fig. 4-9. Power and flow transients in flow blockage accident

2. Cladding begins to melt, flow down the fuel rod, and solidify in the lower axial blanket.

3. If the cladding does not block the lower axial blanket coolant channels, then damage propagation is less likely. STEFINS has calculated blockage for a cladding mass flow rate equivalent to all the cladding of one rod entering the lower axial blanket within 1 s (90 g/s). The SCORIA calculated melt time for 90% of the cladding in the hottest rod is 2 s. Slower mass flow rates more readily cause solidification in the lower axial blanket.

4. Fuel begins to melt at 6 s, slump, and build up upon the steel blockage.

5. The duct wall begins to heat up from contact with molten fuel and begins to melt. At this time about 70% of the fuel has melted in an upflow core and 60% of the fuel has melted in a downflow core. The average pool temperature is about 2927°C.

6. The heat transfer within the molten fuel is treated using recently developed PAFC experimental correlations for convection within molten fuel pools surrounded by cold walls.

7. Reactor trip is assumed to occur from high reactivity at 10 s. This is based on the PSID analysis.

8. It is assumed that the combination of steady-state duct dilation and transient thermal expansion has closed the interduct spacing.

9. The STEFINS program predicts that the duct wall will melt through in about 5 s if the assembly is treated as adiabatic.

10. SCORIA predicts that 10% of full flow after trip in the adjacent assemblies will not prevent duct wall melt-through.

4.4. TRANSIENT OVERPOWER ACCIDENT

This accident encompasses those circumstances in which a power-to-flow mismatch at full-power operation occurs by a postulated reactivity insertion rate with concurrent failure of the plant protection system. It is termed a transient overpower accident, or TOP. Figure 4-10 is a diagram summarizing the expected phenomenological sequence of events and the key uncertainties.

Two possible events which have a major influence on the potential core damage and energetics are (1) fuel-vapor-driven disassembly and (2) recriticality after an initial shutdown. Determination of the occurrence of the former depends on the time and location of cladding failure. Determination of the potential for the latter depends on a detailed knowledge of the fuel motion in the coolant channel after failure. A long time to failure or a failure at or above the core midplane could lead to significant fuel vapor generation and disassembly. Molten fuel refreezing and buildup in the coolant channels could lead to formation of a critical mass in an uncoolable geometry. In this case more extensive core melting and/or vapor-driven disassembly could result. In the event that flow blockages form in the coolant channel, the relative timing of fuel melt-out, fuel boiling, and recriticality would become important. Therefore, issues surrounding the time and location of fuel pin failure and the subsequent fuel motion have provided the direction for most of the study of unprotected TOP accidents to date. The issues regarding fuel sweepout and the permanency of subcriticality after initial fuel motion form the only potentially significant distinction between the upflow and downflow concepts for the TOP.

The potential for fuel re-entry in the downflow core appears remote because both gravity and flow tend to remove the fuel. An uncertainty is the molten or solid fuel fragment size in relation to channel plugging at spacer grid locations. Both concepts face this uncertainty. Furthermore, both concepts should assure that any channel plugging due to released fuel would be such that coolability of the damaged subassemblies could be maintained.

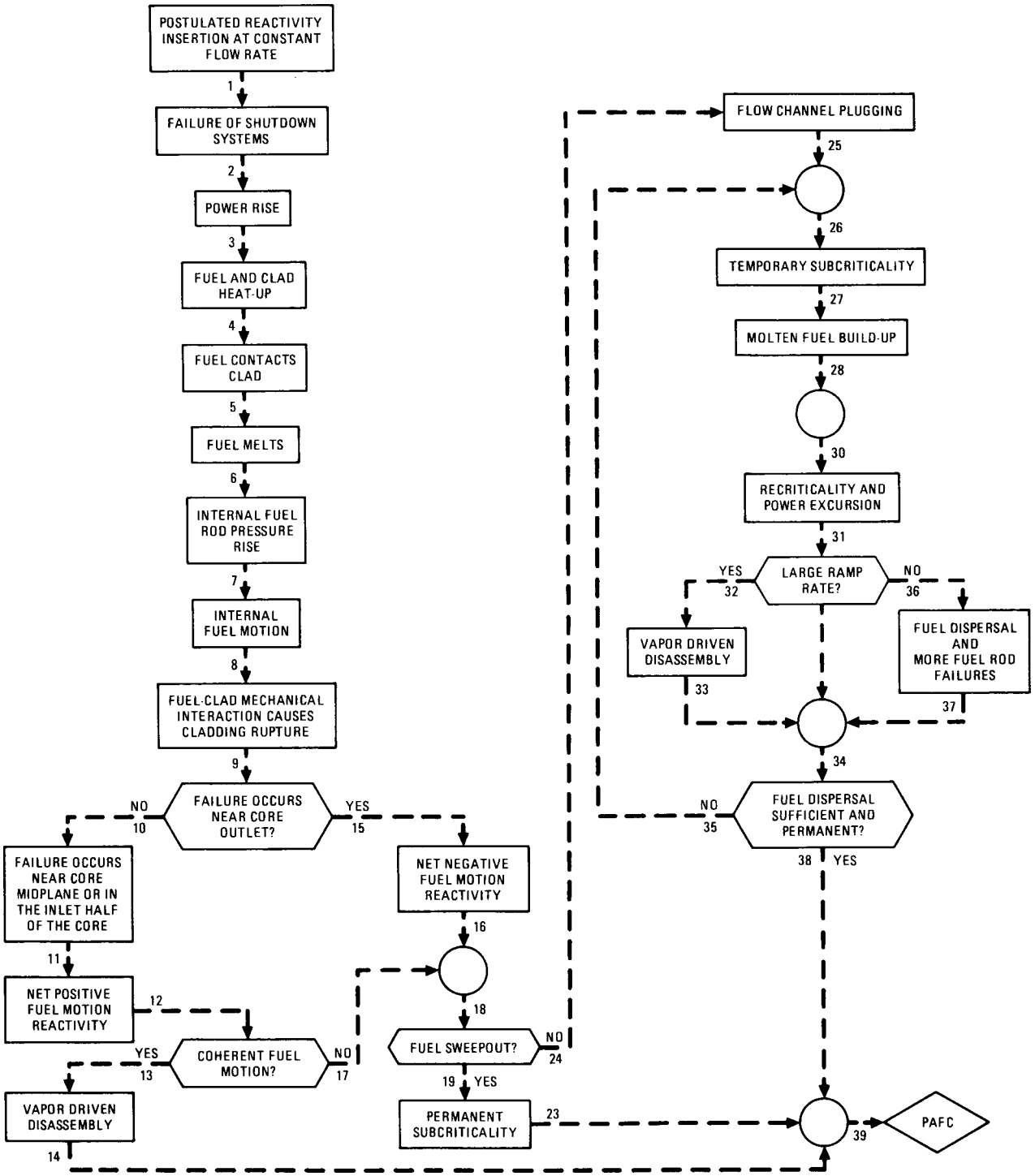

Fig. 4-10. TOP event sequence diagram for the upflow core

It is customary to characterize TOP transients in terms of the input reactivity ramp rates, although Doppler and fuel expansion feedbacks will limit the total feedback. The input ramp rate will determine the rate at which the reactor power rises, which will in turn determine many of the characteristics of the accident. Values which have been considered in the GCFR range from 10¢/s to $10/s.

Regardless of the input ramp rate, the calculated TOP is characterized by a rise in power with an assumed constant coolant flow. For slow ramps, quasi-steady-state thermal conditions would obtain, while for fast ramps, the fuel would heat essentially adiabatically. In either case, the cladding would be subjected to temperature and loading transients that eventually would lead to failure. Potential loading mechanisms include differential thermal expansion of fuel and cladding, loading of cladding by fission gas or dissolved helium gas pressurization, and fuel swelling due to gases entrapped within the fuel. At failure, the fuel pin usually would contain some molten fuel which would be at a high pressure compared with the coolant pressure. When cladding failure occurred, this pressurized molten fuel would be ejected through the breach into the coolant channel. It would then interact hydrodynamically and thermally with the coolant. The nature of this interaction would determine the extent of fuel fragmentation and, to some extent, the subsequent motion. Hydrodynamic and thermal interactions between the coolant, fuel, and channel boundaries would determine the extent to which fuel could undergo sweepout leading to its removal from the reactor core.

Since full coolant flow is calculationally assumed to be maintained, the core damage can be limited if neutronic shutdown can be calculated to occur. Shutdown may be achieved if fuel sweepout occurs in a relatively few subassemblies. Accident termination occurs when the core configuration is subcritical and coolable. Assurance of this mode of accident termination relies on occurrence of several sequential events. First, it is necessary that the time and location of failure be such that initial fuel motion produces shutdown rather than reactivity addition. This means

that failure must occur toward the outlet end of the core after substantial molten fuel generation so that fuel motion will occur promptly upon failure and be away from the core midplane. Second, the sweepout process must be effective so that fuel is removed from the failure site to beyond the core boundaries to ensure permanent subcriticality and to ensure that fuel re-entry does not occur.

Assessment of the energetics of an unprotected TOP accident is closely related to the issues surrounding the extent of core damage. If the arguments leading to shutdown with limited core damage and coolability of damaged assemblies prevail, the accident is energetically benign. However, if the time and location of failure are unfavorable, near the core midplane or toward the inlet, the fuel motion accompanying cladding failure will produce increased reactivity and the potential for an energetic excursion. Furthermore, if permanent fuel removable from the core region is not assured, a second critical configuration may result with subsequent increase in the potential for a core disassembly. Qualitatively, however, it is improbable that a coherent recriticality situation could result from a TOP initiator which would exceed that from an LOF accident.

Because the anticipated event sequence for both the upflow and downflow concepts is very similar for a TOP, it was not a factor in the choice of concept.

4.5. LOSS OF FLOW ACCIDENT COMPARISON

This accident encompasses those circumstances in which concurrent failures in both the primary coolant (main and auxiliary circulators) and reactor shutdown systems are postulated. Flow degradation or coastdown in the core may arise from faults either in the circulation equipment or the high-pressure coolant boundary. It is termed the loss of flow accident,

or LOF. Figure 4-11 is a summary diagram of the expected phenomenological sequence of events and the key uncertainties for the upflow GCFR. The following discussion highlights the differences and similarities between an upflow and a downflow GCFR concept.

Loss of flow accidents starting from full power would proceed to cladding melting but not duct melting prior to fuel melting. The cladding would relocate downward in a downflow core, generating a positive feedback of less than $5/s, and would cause an order of magnitude or more increase in power but would not induce a prompt critical burst. The rate of cladding relocation may be influenced by residual flow during a depressurization or by circulator coastdown. The upflow core would provide a retardation of the rate of downward fuel and cladding relocation due to circulator coastdown, while residual flow in the downflow core would enhance the downward flow of molten material.

The principal uncertainty in an LOF is in the character of subsequent molten fuel motion. Within the phenomena involving fuel motion are the principal distinctions between the hanging and standing core concepts. Depending on the time delay between cladding melting and fuel melting, cladding material may or may not block coolant channels in the lower axial blanket. Complete or nearly complete blockage in either the upflow or downflow core may lead to fuel slumping and fuel boiling.

If fuel melting follows cladding melting close enough in time, then cladding refreezing in the lower axial blanket may not occur. The phenomenon depends on the power level of the particular subassembly. In high-power subassemblies, fuel vaporization within the pellet columns would drive molten fuel rapidly up and down the flow channels. A temporarily subcritical state might be reached because of this early fuel dispersal. However, the dispersal force might cause the remaining intact pellet stacks to buckle and fall. The combination of intermixed molten fuel and steel within a matrix of solid pieces of buckled pellet stacks would cause the fuel/steel mixture to solidify and block lower axial blanket coolant

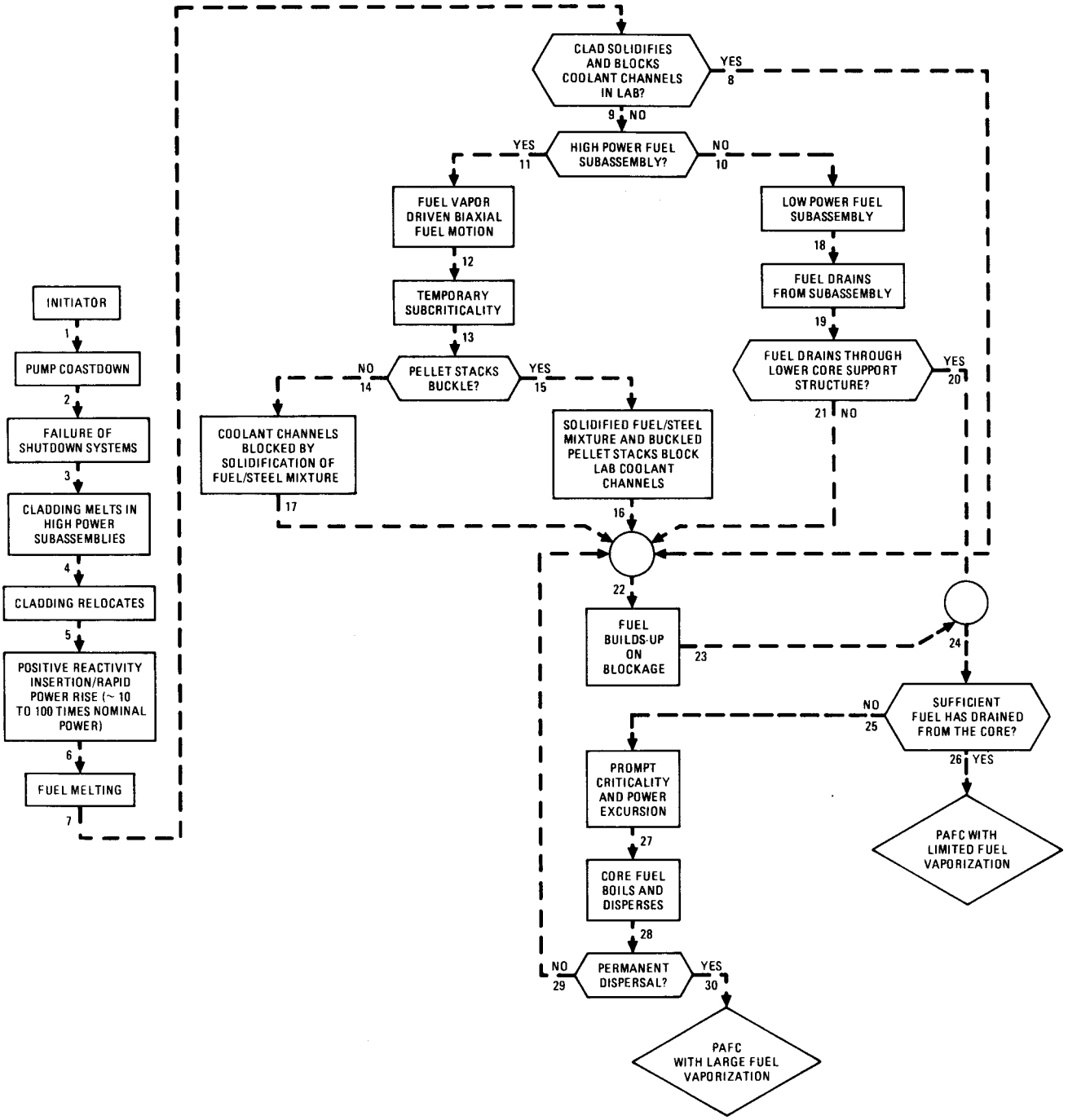

Fig. 4-11. LOF event sequence diagram for the upflow core

channels. The lower axial blanket coolant channels in the high-power subassemblies might be blocked by the solidification of a turbulently mixed fuel/steel combination even without fuel column crumbling. Certain low-power assemblies, on the other hand, may have a combination of melting rates and temperatures which prohibits steel blockages from forming in the lower axial blanket and allows molten fuel to drain through the assembly.

In the event of fuel/steel blockages in the high-power subassemblies and insufficient or delayed drainage, a prompt critical burst and boiled-up core sequence may be expected when the molten fuel which has been driven upward returns. The only accident termination mechanism with this scenario in an upflow core is the vapor-driven dispersal of sufficient fuel to allow the remaining molten fuel to be subcritical.

The ultimate consequences of an LOF (e.g., fraction of fuel vaporized) appear to hinge on the ability to remove fuel from the core. Similar fuel removal avenues appear to be available in either concept.

REFERENCES

4-1. Cha, B. K., G. A. McLellan, and P. J. Fulford, "NUBOW 2D Inelastic: A Fortran Program for Static 2-Dimensional Structural Analysis of Bowed Reactor Cores, Including Effects of Irradiation Creep, Swelling," DOE Report ANL-CT-77-34, Argonne National Laboratory, 1977.

4-2. Dalle Donne, M., S. Dorner, and K. Schretzmann, "Post Accident Heat Removal Considerations for Gas-Cooled Fast Breeder Reactors," NEA Coordinating Group on GCFR Development, Specialist Meeting on Design, Safety and Development of the GCFR, Tokyo, March 1976.

4-3. Kang, C. S., and A. Torri, "Preliminary Analysis of Post-Accident Fuel Containment for a GCFR," DOE Report GA-A14789, General Atomic Company, to be published.

4-4. Baker, L., et al., "Heat Removal from Molten Fuel Pools," Proceedings of the International Meeting on Fast Reactor Safety and Related Physics, October 5-8, 1976, Chicago, Illinois, p. 2056 (CONF-761001).

4-5. Dalle Donne, M., S. Dorner, and G. Schumacher, "Development Work for a Borax Internal Core-Catcher for a Gas-Cooled Fast Reactor," Nucl. Technol. 39, 138-154 (July 1978).

4-6. "Gas-Cooled Fast Breeder Reactor, Quarterly Progress Report for the Period May 1, 1978 through July 31, 1978," DOE Report GA-A15054, General Atomic Company, August 1978.

4-7. "Gas-Cooled Fast Breeder Reactor Quarterly Progress Report for the Period November 1, 1978 through January 31, 1979," DOE Report GA-A15237, General Atomic Company, February 1979.